

Colloquium: Quantum batteries

Francesco Campaioli^{*}

Dipartimento di Fisica e Astronomia “G. Galilei,” Università degli Studi di Padova, I-35131 Padua, Italy, Padua Quantum Technologies Research Center, Università degli Studi di Padova, I-35131 Padua, Italy, and ARC Centre of Excellence in Exciton Science and School of Science, RMIT University, Melbourne 3000, Australia

Stefano Gherardini[†]

CNR-INO, Largo Enrico Fermi 6, I-50125 Firenze, Italy and European Laboratory for Non-linear Spectroscopy, Università di Firenze, I-50019 Sesto Fiorentino, Italy

James Q. Quach[‡]

CSIRO, Ian Wark Laboratory, Bayview Avenue, Clayton, Victoria 3168, Australia and The University of Adelaide, South Australia 5005, Australia

Marco Polini[§]

Dipartimento di Fisica dell’Università di Pisa, Largo Bruno Pontecorvo 3, I-56127 Pisa, Italy, Planckian srl, Pisa, Italy, Istituto Italiano di Tecnologia, Graphene Labs, Via Morego 30, I-16163 Genova, Italy, and ICFO—Institut de Ciències Fotòniques, The Barcelona Institute of Science and Technology, Avinguda Carl Friedrich Gauss 3, 08860 Castelldefels (Barcelona), Spain

Gian Marcello Andolina^{||}

ICFO—Institut de Ciències Fotòniques, The Barcelona Institute of Science and Technology, 08860 Castelldefels (Barcelona), Spain and JEIP, USR 3573 CNRS, Collège de France, PSL Research University, 11 Place Marcelin Berthelot, F-75321 Paris, France

 (published 9 July 2024)

Recent years have witnessed an explosion of interest in quantum devices for the production, storage, and transfer of energy. This Colloquium concentrates on the field of quantum energy storage by reviewing recent theoretical and experimental progress in quantum batteries. Provided first is a theoretical background discussing the advantages that quantum batteries offer with respect to their classical analogs. The existing quantum many-body battery models are then reviewed and a thorough discussion of important issues related to their “open nature” is presented. The Colloquium concludes with a discussion of promising experimental implementations, preliminary results available in the literature, and perspectives.

DOI: [10.1103/RevModPhys.96.031001](https://doi.org/10.1103/RevModPhys.96.031001)

CONTENTS

I. Introduction	2	2. Completely passive states	4
II. Theoretical Background and Methods	3	3. Bounds on extractable and injectable work	4
A. Unitary charging and work extraction	3	4. Entanglement generation and work extraction and injection	4
1. Ergotropy and passive states	4	B. Charging power	5
		1. Average and instantaneous power	5
		2. Bound on the maximal power	5
		C. Quantum advantage	5
		1. Local and global charging	6
		2. Role of entanglement, correlations, and coherence	6
		3. Role of interaction order	7
		4. Genuine quantum advantage	7

^{*}francesco.campaioli@unipd.it

[†]stefano.gherardini@ino.cnr.it

[‡]james.quach@csiro.au

[§]marco.polini@unipi.it

^{||}gian-marcello.andolina@college-de-france.fr

III. Models of Many-Body Batteries	8
A. Charging protocols and figure of merits	8
1. Direct charging protocol	9
2. Charger-mediated protocol	9
B. Charging properties of the Dicke quantum battery	9
1. The Dicke battery	9
2. Parallel versus collective charging	10
3. Origin of the charging advantage	11
4. Charging advantage in the thermodynamic limit	11
5. Variations of the Dicke batteries	12
C. Charging properties of other many-body batteries	13
1. Spin-chain and spin-network batteries	13
2. SYK quantum batteries	13
D. Work extraction	14
IV. Charging Precision	15
A. Bosonic batteries and Gaussian unitaries	15
B. Adiabatic quantum charging	15
C. Entanglement and work fluctuations	16
V. Open Quantum Batteries	17
A. Charging a dissipative quantum battery	17
1. Dissipative charging	17
2. Environment-assisted charging	18
B. Active charging and stabilization methods	18
1. Controllability of closed and open quantum batteries	18
2. Stabilization power and its energy cost	19
3. Charging and stabilization via sequential measurements	19
4. Charging and stabilization with feedback control	20
C. Protection from energy losses	21
1. Protection via decoherence-free subspaces	21
2. Engineering spontaneous dark-state preparation	22
VI. Experimental Implementations	23
A. Superconductors	23
B. Quantum dots	23
C. Organic microcavities	23
D. Nuclear spins	24
VII. Conclusions and Outlook	24
Acknowledgments	25
References	25

I. INTRODUCTION

Developments in the field of quantum information have generated great expectations that quantum effects like entanglement could be exploited to perform certain tasks with sizable advantages over classical devices (Horodecki *et al.*, 2009). Theoretical examples for the existence of such advantages have led to considerable research and industry operations in the fields of computations (Ladd *et al.*, 2010; Fedorov *et al.*, 2022), cryptography (Gisin *et al.*, 2002; Portmann and Renner, 2022), and sensing (Giovannetti, Lloyd, and Maccone, 2011; Degen, Reinhard, and Cappellaro, 2017). The emergence of new quantum technologies based on these effects is expected to eventually lead to a disruptive technological revolution (Acín *et al.*, 2018).

In the past, technological revolutions were driven by the development of a new scientific theory. Two centuries ago, the success of the first industrial revolution was deeply intertwined with the development of thermodynamics (Carnot, 1824; Fermi, 1956). As an empirical theory based on laws postulated from experience (Fermi, 1956), thermodynamics has a universal

character, offering predictions that are valid for both classical and quantum settings. For example, just as heat cannot naturally flow from a cold to a hot bath, the efficiency of a heat engine based on a quantum system cannot surpass the Carnot limit. Analogously, entanglement cannot be used to extract more work from a thermal energy reservoir (Hovhannisyan *et al.*, 2013). Thus, at first glance there seems to be no place for a quantum advantage in thermodynamics.

However, thermodynamics at equilibrium does not set bounds on how fast energy is transformed into heat and work. Therefore, it is natural to seek thermodynamic quantum advantages in quantum systems that are driven out of equilibrium (Vinjanampathy and Anders, 2016; Binder *et al.*, 2018). Groundbreaking theoretical results in the field of quantum thermodynamics have shown that entanglement generation is linked to faster work extraction when energy is stored in many-body quantum systems (Hovhannisyan *et al.*, 2013). These and other results have sparked interest in quantum systems used as heat engines (Kieu, 2004; Uzdin, Levy, and Kosloff, 2016) and energy storage devices. This led to the emergence of research on quantum batteries, formally introduced by Alicki and Fannes (2013), and the search for quantum effects that improve their performance (Binder *et al.*, 2015b; Campaioli *et al.*, 2017).

Like electrochemical batteries, quantum batteries are temporary energy storage systems. They have a finite energetic capacity and power density (Julià-Farré *et al.*, 2020) and can lose energy to the environment (Liu, Segal, and Hanna, 2019; Gherardini *et al.*, 2020). However, quantum batteries can be charged (or expended) via operations that generate coherent superpositions between different states (Binder *et al.*, 2015a). In quantum batteries composed of many subcells, these coherences can form entanglement and other nonclassical correlations (Campaioli *et al.*, 2017), leading to a super-extensive scaling of the charging power. This quantum effect, which is akin to the Heisenberg scaling in quantum metrology and that of Grover’s search algorithm, leads to an advantage over classical devices and has thus been one of the main driving forces of this field.

A major boost to this research field occurred when Ferraro *et al.* (2018) showed that a quantum battery based on the Dicke model¹ (Dicke, 1954) could achieve a superextensive power scaling. Since this finding, many other quantum battery models have been theoretically proposed, from one-dimensional spin chains (Le *et al.*, 2018) to strongly interacting Sachdev-Ye-Kitaev fermionic batteries (Rossini *et al.*, 2020). More recently important but preliminary steps toward the experimental implementation of quantum batteries have also been made (Hu *et al.*, 2022; Joshi and Mahesh, 2022; Quach *et al.*, 2022).

Meanwhile, theoretical studies have clarified the role of quantum correlations and collective effects toward achieving superextensive power scaling (Campaioli *et al.*, 2017; Andolina *et al.*, 2018; Julià-Farré *et al.*, 2020; Gyhm,

¹The Dicke model can be engineered in solid-state and other quantum architectures. Its energy storage properties were studied by Fusco, Paternostro, and De Chiara (2016), Ferraro *et al.* (2018), Crescente *et al.* (2020a), Dou *et al.* (2022), and Gemme *et al.* (2023).

Šafránek, and Rosa, 2022), i.e., a charging power that grows faster than the number of subcells. Recent studies have also proposed protocols to maximize charging efficiency and precision (Friis and Huber, 2018; Santos *et al.*, 2019; Rosa *et al.*, 2020) and methods to prevent energy loss due to the environment (Liu, Segal, and Hanna, 2019; Gherardini *et al.*, 2020; Quach and Munro, 2020; Mitchison, Goold, and Prior, 2021; Hernández-Gómez *et al.*, 2022). However, many aspects of the physics of quantum batteries remain unexplored, such as the ultimate limits on energy density, absolute power, and the lifetime of energy storage (Mohan and Pati, 2021). Furthermore, experimental work on quantum batteries is still in its infancy, and a fully operational proof of principle is yet to be demonstrated.

This Colloquium aims to be a self-contained, pedagogical review of this rapidly developing field. In Sec. II, we introduce the theoretical framework to study quantum batteries and look at theorems and bounds of general validity. We then examine the most prominent models of quantum batteries in Sec. III, focusing on the superextensive scaling of the charging power. The effect of work fluctuations on the precision of charging and work extraction protocols are reviewed in Sec. IV. We then review approaches for charging and stabilization in the presence of decoherence and energy-loss processes in Sec. V. In Sec. VI, we survey the most promising platforms for the experimental realization of quantum batteries. With the aim of providing scope and momentum to this emerging research field, we conclude by presenting in Sec. VII an overview of urgent research questions.

II. THEORETICAL BACKGROUND AND METHODS

A. Unitary charging and work extraction

In their seminal work, Alicki and Fannes (2013) defined a quantum battery as a d -dimensional system whose internal Hamiltonian H_0 (or bare Hamiltonian) has nondegenerate energy levels ($\epsilon_k < \epsilon_{k+1}$),

$$H_0 = \sum_{k=1}^d \epsilon_k |k\rangle\langle k|. \quad (1)$$

In Eq. (1) we relax this condition by allowing partial degeneracy ($\epsilon_k \leq \epsilon_{k+1}$) as long as the Hamiltonian H_0 has a nonzero bandwidth² $w[H_0] := \epsilon_{\max} - \epsilon_{\min} > 0$, where ϵ_{\max} (ϵ_{\min}) is the largest (smallest) eigenvalue.³ Energy can be stored in this system by preparing it in some excited state ρ such that its energy $\text{Tr}[H_0\rho] > \epsilon_1$. Examples of quantum systems that can be used as quantum batteries include (but are not limited to) spins in a magnetic field (Le *et al.*, 2018), semiconductor quantum dots (Wenniger *et al.*, 2022), superconducting qubits (Santos *et al.*, 2019; Dou, Wang, and Sun, 2022a), the electronic states of an organic molecule (Liu and Hanna, 2018; Quach *et al.*, 2022), and the states of the

electromagnetic field confined in a high-quality photonic cavity (Friis and Huber, 2018).

In contrast with its classical counterpart, a quantum battery can be charged via unitary operations that may temporarily generate coherences between its eigenstates $|k\rangle$. Besides minimizing heat production, unitary charging can generate nonclassical correlations in many-body quantum batteries, leading to the superextensive charging power scaling discussed in Secs. II.B.1 and III.

For the moment, we focus on the amount of energy that can be reversibly injected (charging) or extracted (discharging) via a cyclic unitary process,

$$\dot{\rho}(t) = -i[H_0 + H_1(t), \rho(t)], \quad (2)$$

where $H_1(t)$ is a Hermitian time-dependent interaction that is turned on at time $t=0$ and off at time $t=\tau$ and $\dot{\rho}(t)$ represents the time derivative of $\rho(t)$, with $\rho_0 := \rho(0)$. Note that \hbar is set to 1 unless otherwise specified. The energy W deposited in such a way is measured with respect to the internal Hamiltonian H_0 ,

$$W(\tau) = \text{Tr}[H_0\rho(\tau)] - \text{Tr}[H_0\rho_0], \quad (3)$$

where $\rho(\tau) = U(\tau; 0)\rho_0 U^\dagger(\tau; 0)$ is obtained from the solution of Eq. (2), with $U(t; 0) = \mathcal{T}(\exp\{-i\int_0^t ds [H_0 + H_1(s)]\})$ the time-evolution operator expressed in terms of the time-ordering operator \mathcal{T} . If we restrict ourselves to unitary evolution, work injection (charging) and extraction are effectively equivalent tasks. More precisely the work extracted from the system W_{out} is related to the energy deposited W_{in} by the relation $W_{\text{in}} = -W_{\text{out}}$, where W_{in} is obtained as in Eq. (3). The subscripts are often omitted here to simplify the notation.

The processes of reversible charging and work extraction are illustrated in Fig. 1 in relation to those of energy loss

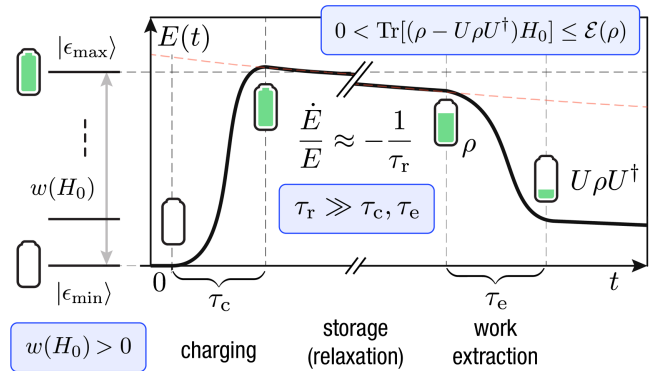


FIG. 1. A quantum battery is a quantum system with nonzero energy bandwidth $w(H_0) = \epsilon_{\max} - \epsilon_{\min} > 0$. Charging and work extraction can be performed by means of cyclic unitary operations, as prescribed by Eq. (2). An active state ρ (i.e., a nonpassive state) and a unitary operation U are needed, so some work $\text{Tr}[(\rho - U\rho U^\dagger)H_0] > 0$ can be extracted from the system. Optimally U extracts the ergotropy $\mathcal{E}(\rho)$, defined in Eq. (4). In practice, a quantum battery may lose energy at some relaxation rate τ_r^{-1} due to the interaction with the environment, as discussed in Sec. V. Ideally charging or extraction and relaxation timescales should be well separated ($\tau_r \gg \tau_c, \tau_e$).

²Corresponding to the maximal amount of energy that can be stored in the system.

³ $w[H_0] := \epsilon_d - \epsilon_1$ for nondegenerate spectra.

(or leakage), as discussed in Sec. V. We now introduce some figures of merit and key concepts by gradually introducing the fundamental relation between charging power and the formation of quantum correlations, which is later reviewed in Sec. II.B.

1. Ergotropy and passive states

Restricting the dynamics to unitary cycles imposes a bound on the amount of energy that can be deposited or extracted via Eq. (2). This observation leads to the definition of *ergotropy* (Allahverdyan, Balian, and Nieuwenhuizen, 2004), denoted by \mathcal{E} or W_{\max} , as the maximal amount of work that can be extracted from a state ρ via unitary operations,

$$\mathcal{E}(\rho) := \text{Tr}[H_0\rho] - \min_{U \in \text{SU}(d)} \{\text{Tr}[H_0 U \rho U^\dagger]\}. \quad (4)$$

In Eq. (4) the minimization is performed with respect to unitary operators U in the special unitary group $\text{SU}(d)$. As such, the ergotropy is one of the key figures of merit for the performance of quantum batteries (Sone and Deffner, 2021; Tirone, Salvia, and Giovannetti, 2021; Touil, Çakmak, and Deffner, 2022).

When no work can be extracted from some state, such a state is called *passive*. In other words, a state σ is passive when $\text{Tr}[H_0\sigma] \leq \text{Tr}[H_0 U \sigma U^\dagger]$ for all unitaries U . It turns out that σ is passive if and only if it is diagonal in the basis of the Hamiltonian H_0 , and its eigenvalues are nonincreasing with the energy (Lenard, 1978; Pusz and Woronowicz, 1978; Salvia and Giovannetti, 2021; Mazzoncini *et al.*, 2023),

$$\sigma = \sum_{k=1}^d s_k |k\rangle\langle k|, \quad s_{k+1} \leq s_k. \quad (5)$$

For any state $\rho = \sum_k r_k |k\rangle\langle k|$, there is a unique⁴ passive state σ_ρ that minimizes the term $\text{Tr}[H_0 U \rho U^\dagger]$ in Eq. (4). The state σ_ρ is obtained via some unitary operation U_ρ that sorts the eigenvalues of ρ in nonincreasing order $\{r_k\} \rightarrow \{r'_k\}$ such that

$$\sigma_\rho = U_\rho \rho U_\rho^\dagger = \sum_{k=1}^d r'_k |k\rangle\langle k|. \quad (6)$$

Accordingly the ergotropy can be expressed in terms of such a passive state as $\mathcal{E}(\rho) = \text{Tr}[H_0\rho] - \text{Tr}[H_0\sigma_\rho]$.

As one would expect from Eq. (5), all thermal states⁵ $G_\beta = \exp[-\beta H_0]/\mathcal{Z}$ are passive since they commute with H_0 and their eigenvalues do not increase with energy. Less trivial is the fact that the ergotropy of some state ρ is upper bounded as

$$\mathcal{E}(\rho) \leq \text{Tr}[H_0\rho] - \text{Tr}[H_0 G_{\bar{\beta}}], \quad (7)$$

⁴If H_0 has a nondegenerate spectrum.

⁵In G_β , $\beta = 1/k_B T$ is the inverse temperature, or inverse thermal energy, $\mathcal{Z} = \text{Tr} \exp[-\beta H_0]$, and k_B is the Boltzmann constant.

where $\bar{\beta}$ is such that ρ and $G_{\bar{\beta}}$ have the same von Neumann entropy $S(\rho) = -\text{Tr}[\rho \log \rho] = S(G_{\bar{\beta}})$ (Alicki and Fannes, 2013).

Since every state of a two-level system (TLS) can be seen as a thermal state, when $d = 2$ all passive states are thermal and Eq. (7) becomes a tight bound. In general, passive states may not be thermal, and finding σ_ρ effectively becomes a sorting problem in the eigenbasis of the Hamiltonian H_0 , whose computational complexity typically scales as $O(d \log d)$ (Zutshi and Goswami, 2021).

2. Completely passive states

A key question in quantum thermodynamics is to determine whether or not quantum phenomena like coherence (Francica *et al.*, 2020) and entanglement can be harnessed in some thermodynamics task (Binder *et al.*, 2018). To address this question, Alicki and Fannes (2013) considered the case of composite systems with N constituents and focused on states of the form $\otimes^N \rho := \otimes_{j=1}^N \rho$, i.e., states that are given by N copies of the same state ρ . They considered a system whose Hamiltonian $H_0^{(N)}$ is given by N local copies of H_0 ,

$$H_0^{(N)} = \sum_{i=1}^N H_i, \quad (8)$$

where $H_i := \mathbb{1}_1 \otimes \cdots \otimes \mathbb{1}_{i-1} \otimes H_0 \otimes \mathbb{1}_{i+1} \cdots \otimes \mathbb{1}_N$. This system can be seen as a quantum battery given by N noninteracting cells.⁶ In Secs. III and VI we discuss possible experimental implementations of such a Hamiltonian.

Note that N copies of a passive state may not form a passive state with respect to $H_0^{(N)}$. It therefore makes sense to define a subclass of passive states that are called *completely passive*. These are N -copy states that are passive for any N . Notably a state ρ is completely passive if and only if it is thermal (Lenard, 1978).

3. Bounds on extractable and injectable work

Using the aforementioned result, Alicki and Fannes (2013) showed that the bound in Eq. (7) could be achieved asymptotically in the $N \rightarrow \infty$ limit for systems with N constituents. Given an N -copy state $\otimes^N \rho$, the ergotropy per copy $\varepsilon(N)$ is defined as

$$\varepsilon(N) := \frac{1}{N} \{\text{Tr}[H_0^{(N)} \otimes^N \rho] - \text{Tr}[H_0^{(N)} \sigma_{\otimes^N \rho}]\}. \quad (9)$$

In the $N \rightarrow \infty$ limit, $\varepsilon(N)$ is tightly bounded as in Eq. (7), $\lim_{N \rightarrow \infty} \varepsilon(N) = \text{Tr}[H_0\rho] - \text{Tr}[H_0 G_{\bar{\beta}}]$, which follows from the fact that the energy difference between the passive state of the copies $\sigma_{\otimes^N \rho}$ and $\otimes^N G_{\bar{\beta}}$ vanishes in the limit $N \rightarrow \infty$ (Alicki and Fannes, 2013).

4. Entanglement generation and work extraction and injection

Since the passive state of the copies $\sigma_{\otimes^N \rho}$ is diagonal in the eigenbasis of the local Hamiltonian $H_0^{(N)}$, it follows that it is

⁶Note that in general $H^{(N)}$ will have degenerate eigenvalues.

also separable.⁷ However, using local operations (here permutations⁸) of the eigenvalues of $\otimes^N \rho$, we can reach only $\otimes^N \sigma_\rho$ at best. Therefore, to extract the ergotropy (or, equivalently, to inject the anti-ergotropy) one must use *entangling* operations, i.e., operations that can generate entanglement between two or more subsystems.

This observation led [Alicki and Fannes \(2013\)](#) to suggest that entanglement generation is needed for optimal reversible work extraction. However, it was later shown by [Hovhannisyán *et al.* \(2013\)](#) that the ergotropy can in fact be extracted from N copies of ρ while keeping their state separable at all times as long as at least two-body operations are available. They showed that entanglement generation can always be avoided by taking a longer unitary trajectory. The results of [Hovhannisyán *et al.* \(2013\)](#) hinted at a relation between entanglement generation and power, and in the process answered the key questions of Sec. II.A.2 and led the way toward the quantitative study of such a relation.

B. Charging power

1. Average and instantaneous power

[Binder *et al.* \(2015b\)](#) proposed shifting the focus from work extraction to charging. They considered the average charging power $\langle P \rangle_\tau$ of some unitary process as the ratio between the average deposited energy $W(\tau)$ and the time τ required to complete the procedure. Let $P(t) := \dot{W}(t)$ be the instantaneous power

$$P(t) = \text{Tr}[H_0 \dot{\rho}(t)] \quad (10)$$

intended as time-local energy gain with respect to the time-independent internal Hamiltonian of the battery. The average power is then given by

$$\langle P \rangle_\tau = \frac{W(\tau)}{\tau}, \quad (11)$$

where $\langle f \rangle_\tau$ denotes the time average of some function $f(t)$ in the time interval $t \in [0, \tau]$, i.e., $\langle f \rangle_\tau := (1/\tau) \int_0^\tau dt f(t)$. For simplicity, we often omit the subscript τ in $\langle P \rangle_\tau$ in the Colloquium and assume the implicit dependence of the average power on the time interval over which it is calculated.

In practical applications, it is desirable for charging to be as fast as possible. [Binder *et al.* \(2015b\)](#) therefore sought to maximize the average power $\langle P \rangle$. Alternatively, they proposed studying a family of objective functions $\mathcal{F}_\alpha[P, W] := \langle P \rangle^\alpha \langle W \rangle^{1-\alpha}$ with $0 \leq \alpha \leq 1$ to balance between work and power outputs.

2. Bound on the maximal power

To seek a bound on the average power $\langle P \rangle$, [Binder *et al.* \(2015b\)](#) formulated the charging problem in terms of finding

⁷A state ρ is separable if it is a convex of combination of the product states ([Mintert *et al.*, 2005](#)).

⁸Local permutations are permutations of the eigenvalues of each individual copy ρ .

the minimal time required to reach some target state ρ^* starting from some initial state ρ_0 by means of unitary evolution. This problem, which is known as the quantum speed limit (QSL) ([Giovannetti, Lloyd, and Maccone, 2003](#); [Deffner and Lutz, 2013](#); [Deffner and Campbell, 2017](#)), has been studied as an operational interpretation of time-energy uncertainty relations ([Campaioli, 2020](#)). When one considers pairs of pure states $|\psi\rangle$ and $|\phi\rangle$, the minimal time τ required to unitarily evolve between them is given by the unified bound ([Mandelstam and Tamm, 1945](#); [Margolus and Levitin, 1998](#); [Levitin and Toffoli, 2009](#); [Deffner and Lutz, 2013](#))

$$\tau \geq \tau_{\text{QSL}} = \frac{\arccos |\langle \psi | \phi \rangle|}{\min\{\langle E \rangle, \langle \Delta E \rangle\}}, \quad (12)$$

where $\langle E \rangle$ and $\langle \Delta E \rangle$ are the time-averaged expectation value and the standard deviation of the total Hamiltonian $H(t) = H_0 + H_1(t)$. These are calculated from $E(t) = \text{Tr}[H(t)\rho(t)] - \omega_1(t)$, where $\omega_1(t)$ is the instantaneous ground-state energy of $H(t)$ and $\Delta E(t) = \sqrt{\text{Tr}[H^2(t)\rho(t)] - \text{Tr}[H(t)\rho(t)]^2}$ ([Deffner and Lutz, 2013](#)). Equation (12) is attainable for the evolution of pure states for any $H_1(t)$ of Eq. (2). A prescription for the interaction Hamiltonian $H_1(t)$ to saturate the bound is

$$H_1(t) = \lambda(t)[-H_0 + \alpha|\psi\rangle\langle\phi| + \alpha^*|\phi\rangle\langle\psi|], \quad (13)$$

where $\lambda(t) = 1$ for $0 < t \leq \tau$ and zero otherwise for orthogonal pairs of states, where α is a nonzero complex number. By imposing $H_1(t)$ to have finite energy, for example, via the operator norm $\|H(t)\| = E_{\text{max}}$ for some $E_{\text{max}} > 0$, the minimal evolution time becomes $\tau = \pi/2E_{\text{max}}$. From this result, [Binder *et al.* \(2015b\)](#) concluded that the following inequality must be true:

$$\langle P \rangle \leq 2WE_{\text{max}}/\pi, \quad (14)$$

when considering a charging process between orthogonal states associated with an injection of energy W . The right-hand side of the bound in Eq. (14) has units of power, provided that \hbar is reintroduced.

C. Quantum advantage

We now review how a quantum advantage can be achieved for the task of charging a quantum battery. To seek a formal definition, we consider a figure of merit Γ that is built in such a way that $\Gamma > 1$ when a quantum advantage is achieved. A first formulation was given by [Campaioli *et al.* \(2017\)](#),

$$\Gamma := \frac{\langle P_q \rangle}{\langle P_c \rangle}. \quad (15)$$

In Eq. (15) $\langle P_q \rangle$ ($\langle P_c \rangle$) represents the maximal charging power of a quantum (classical) charging protocol.

While the distinction between quantum and classical is loose here, initial consensus on this definition was based on the idea that a charging protocol is quantum mechanical when it generates nonclassical correlations ([Campaioli *et al.*, 2017](#); [Ferraro *et al.*, 2018](#); [Le *et al.*, 2018](#)) like entanglement and

quantum discord (Modi *et al.*, 2011). Nevertheless, the notion of an advantage that is genuinely quantum mechanical is still under investigation (Andolina, Keck, Mari, Giovannetti, and Polini, 2019; Rossini *et al.*, 2020); see Sec. II.C.4.

1. Local and global charging

We now again consider the quantum battery given by the composite system with Hamiltonian $H_0^{(N)}$ defined in Eq. (8). When depositing energy onto such a system by means of some unitary process, we can consider two different scenarios: (i) local charging if each subsystem is charged independently and (ii) global⁹ charging if the control interaction couples different subsystems. In this scenario, it is insightful to consider a charging task $|G\rangle \rightarrow |E\rangle$, which deposits some energy W from the N -copy passive state $|G\rangle := \otimes^N |g\rangle$ (a *dead* battery) to the active state $|E\rangle := \otimes^N |e\rangle$ (a *charged* battery), where $|g\rangle := |1\rangle$ and $|e\rangle := |d\rangle$ are the ground and excited states of the d -dimensional system defined in Eq. (1).

If we can only use local interactions, the best approach to achieve the $|G\rangle \rightarrow |E\rangle$ task is to drive each subsystem independently at the QSL. This can be done using the local (i.e., one-body interactions only) charging Hamiltonian

$$H_{\parallel}^{(N)} = \sum_{i=1}^N V_i, \quad (16)$$

where each V_i is a local copy of $-H_0 + \alpha|e\rangle\langle g| + \alpha^*|g\rangle\langle e|$ acting on the subsystem i , as discussed in Sec. II.B.2. If instead we can use arbitrary N -body interactions, the best approach is to use the global Hamiltonian (Binder *et al.*, 2015b)

$$H_{\parallel}^{(N)} = -H_0^{(N)} + \alpha_N|E\rangle\langle G| + \alpha_N^*|G\rangle\langle E|. \quad (17)$$

To make a fair comparison between these two charging approaches, we impose that both Hamiltonians have the same operator norm, i.e., that $\|H_{\parallel}^{(N)}\| = \|H_{\parallel}^{(N)}\| = E_{\max}$. We then obtain $E_{\max} = |\alpha_N| = N|\alpha|$, which implies the minimal time of local charging is $\tau_{\parallel} = N\pi/2E_{\max}$, that is, N times larger than that of global charging $\tau_{\parallel} = \pi/2E_{\max}$. We then arrive at an explicit expression for the quantum advantage of this charging task,

$$\Gamma = \frac{\langle P_{\parallel} \rangle}{\langle P_{\parallel} \rangle} = \frac{\tau_{\parallel}}{\tau_{\parallel}} = N. \quad (18)$$

Since the global Hamiltonian generates entanglement between the subsystems during the charging process, Binder *et al.* (2015b) concluded that entanglement generation was responsible for the N -fold speedup and necessary to obtain some nontrivial advantage $\Gamma > 1$.

⁹Local and global are otherwise referred to as *parallel* and *collective* in some references. Here we use global for generality to make a distinction between collective and quantum advantage, as discussed in Sec. II.C.4.

However, as discussed in Sec. II.C.2, a quantum advantage can be achieved even without generating entanglement, at the price of reducing the amount of energy extracted or injected (Campaioli *et al.*, 2017). In recent years, the nature of the advantage $\Gamma > 1$ has been explored by many (Andolina *et al.*, 2018; Andolina, Keck, Mari, Giovannetti, and Polini, 2019; Farina *et al.*, 2019; Andolina, 2020; Julià-Farré *et al.*, 2020; Rossini *et al.*, 2020; Fan, Wu, and Yu, 2021; Abah *et al.*, 2022; Carrasco *et al.*, 2022; Shaghaghi *et al.*, 2023). In the remainder of this section we review the main results of these research efforts while aiming to clarify the role that quantum correlations, coherences, and many-body interactions have on Γ .

2. Role of entanglement, correlations, and coherence

With an explicit example, Campaioli *et al.* (2017) proved that it is possible to achieve an advantage that scales with a power law of N , like that in Eq. (18) even without generating entanglement, at the cost of dramatically reducing the amount of energy injected (or extracted). The example involves an initial completely passive N -copy state $\rho_0 = \otimes^N G_{\beta}$ for some inverse temperature β and its corresponding active state $\rho^* = \otimes^N G_{-\beta}$, both of which were calculated with respect to the local internal Hamiltonian H_0 . By choosing a sufficiently small $\beta > 0$, the state ρ_0 is within the region of the states space known as the *separable ball* (Aubrun and Szarek, 2006). The latter is a spherically symmetric region of the space of states that is centered on the maximally mixed state and that contains only separable states. Any unitary charging procedure that drives ρ_0 to ρ^* will keep $\rho(t)$ within the separable ball at all times. Nevertheless, the charging power of the time-optimal global Hamiltonian is N -fold¹⁰ larger than that of the local optimal Hamiltonian. However, in this case no entanglement is generated during the evolution.

Two remarks are in order. First, while the power advantage is still scalable (i.e., it yields a power that scales with N^2), the total deposited energy and the absolute charging power reduce as β decreases. In other words, the closer ρ_0 is to the maximally mixed state, the less energy will be extractable from ρ^* (Campaioli *et al.*, 2017). Since the separable ball is a comparatively small region of the space of states (Gurvits and Barnum, 2005), achieving quantum advantage without entanglement generation comes at the cost of a considerable reduction in the exchanged work $W = \text{Tr}[H_0(\rho_{\star} - \rho_0)]$. This example shows the importance of entanglement, which must be generated for speedup with pure states and without degradation. Second, this type of Hamiltonian is known to produce *quantum discord* (Modi *et al.*, 2011; Giorgi and Campbell, 2015; Niedenzu, Huber, and Boukobza, 2019), which need not vanish for separable states. The role of entanglement and coherence in the charging process was also explored by Caravelli *et al.* (2020), Kamin, Tabesh, Salimi, and Santos (2020), Shi *et al.* (2022), and Yang *et al.* (2023).

¹⁰When using a constraint on the operator norm of the charging Hamiltonian, as described in Sec. II.C.1.

3. Role of interaction order

The examples considered thus far to achieve $\Gamma = N$ require the use of N -body interactions, i.e., interactions that directly couple N subsystems. However, the vast majority of physical systems display at most two-body interactions, with a few exceptions such as the three-body (Efimov) interaction in nuclear (Naidon and Endo, 2017) and atomic systems (Roy *et al.*, 2013). It is therefore important to determine whether a quantum advantage can be achieved with such limitations on the Hamiltonian. To address this question, Campaioli *et al.* (2017) examined the scaling of Γ for N -body systems when the charging Hamiltonian is limited to k -body interactions, where k is sometimes referred to as the interaction order. They showed that, for composite systems with local internal Hamiltonians $H_0^{(N)}$, the quantum advantage is bounded as

$$\Gamma < \gamma[k^2(m-1) + k], \quad (19)$$

where γ is a constant that does not depend on N and the participation number m is the number of subsystems that are coupled with a given subsystem; see Fig. 2. They also conjectured that $\Gamma < \gamma k$ for an arbitrary k -body Hamiltonian, sparking work to determine the properties of the charging Hamiltonian required to achieve a scalable power advantage (Andolina *et al.*, 2018; Ferraro *et al.*, 2018; Le *et al.*, 2018; Andolina, Keck, Mari, Campisi *et al.*, 2019; Farina *et al.*, 2019).

Recently Gyhm, Šafránek, and Rosa (2022) demonstrated that a scalable quantum advantage for the charging power cannot be achieved without global operations. They bounded the instantaneous power $P(t)$ using the norm of the commutator that generates the evolution $|P(t)| \leq \|[H_0, H_1(t)]\|$ for composite systems of batteries driven by Hamiltonians with at most k -body interactions. They obtained a tight bound for the quantum advantage $\Gamma \leq \gamma k$, where γ does not depend on N and k . In Secs. II.C.4 and III.C.2 we discuss some proposed approaches to achieve a quantum advantage that scales with a power law of N , such as quantum batteries based on the

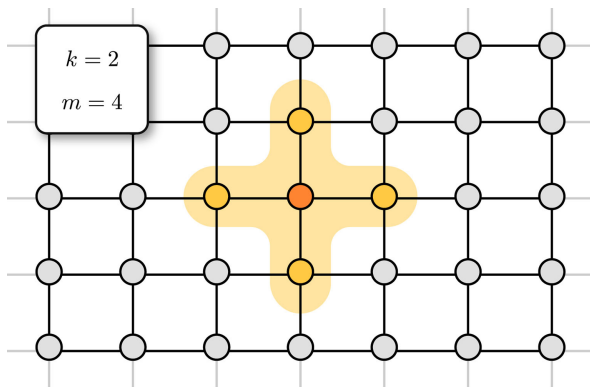


FIG. 2. The bound on the quantum advantage of Eq. (19) depends on the interaction order k (the number of subsystems directly coupled by some interaction) and the participation number m (the number of subsystems that are coupled with any given subsystem). In the 2D lattice with nearest-neighbor interaction shown here, each subsystem directly interacts via pairwise interactions ($k = 2$) with at most four other neighbors ($m = 4$). Adapted from Campaioli, 2020.

Sachdev-Ye-Kitaev (SYK) model (Rossini *et al.*, 2020; Kim *et al.*, 2022).

4. Genuine quantum advantage

The results on the role that entanglement and other quantum correlations have on charging and extraction power have provoked a discussion around the definition of the quantum advantage Γ . Andolina *et al.* (2018) presented a new figure of merit to fairly compare quantum protocols against classical ones, unlike that of Eq. (15). Andolina *et al.* (2018) aimed to quantitatively distinguish charging speedups emerging from many-body interactions from those that stem from the quantum-mechanical nature of the system. They proposed that an unbiased comparison can be made only when a quantum system defined by some Hamiltonian H admits a classical analog \mathcal{H} .

If the dynamics of the quantum system is governed by Eq. (2), that of the classical system is governed by Hamilton's equations of motion,

$$\dot{q}_i = \partial_{p_i} \mathcal{H}, \quad \dot{p}_i = -\partial_{q_i} \mathcal{H}. \quad (20)$$

In Eqs. (20) \vec{q} and \vec{p} are a set of canonically conjugated variables (coordinates and momenta, respectively) such that $\{q_i, p_j\} = \delta_{ij}$, where $\{\cdot, \cdot\}$ denotes the Poisson brackets. Thus, Andolina *et al.* (2018) suggested measuring the advantage stemming from genuine quantum-mechanical effects by comparing the power scaling of the quantum and classical Hamiltonians H and \mathcal{H} , respectively, i.e.,

$$R := \frac{\Gamma_q}{\Gamma_c}. \quad (21)$$

Charging protocols that yield $R > 1$ are said to be characterized by a genuine quantum advantage. In Eq. (21) $\Gamma_q = \langle P_{\#} \rangle / \langle P_{\parallel} \rangle$ represents the advantage of using global operations over local ones, as in Eq. (18), and Γ_c is the same quantity but calculated for the corresponding classical model.

The ratio R has been studied for a variety of charging models (Andolina *et al.*, 2018; Andolina, Keck, Mari, Campisi *et al.*, 2019; Farina *et al.*, 2019; Andolina, 2020; Fan, Wu, and Yu, 2021; Abah *et al.*, 2022; Carrasco *et al.*, 2022; Mondal and Bhattacharjee, 2022). This ratio depends on the model and its microscopic parameters. Note that R is well defined only for quantum battery models that admit a classical analog. There are plenty of models of quantum batteries that do not have a classical analog such as the SYK model considered by Rossini *et al.* (2020) and discussed in Sec. III.C.2. In these cases, it is not possible to evaluate R , and any advantage $\Gamma > 1$ is expected to be stemming from the underlying quantum many-body dynamics (Rossini *et al.*, 2020).

A crucial step in disentangling the contribution of collective interactions from that of quantum correlations was made by Julià-Farré *et al.* (2020). They separated the two contributions using a geometric approach where the instantaneous charging power $P(t)$ was studied. To begin, they noticed that the quantum Fisher information (Barndorff-Nielsen and Gill, 2000) was related to the speed in the Hilbert space (I_Q) and the speed in the energy eigenspace (I_E), while the variance

of the battery Hamiltonian $\Delta E_B^2 = \text{Tr}[H_B^2 \rho_B] - \text{Tr}[H_B \rho_B]^2$ encoded nonlocal correlations between subsystems. Note that if the battery Hamiltonian H_B is made of a sum of local terms $H_B = \sum_{i=1}^N h_i$, it is possible to write $\Delta E_B^2 = \Delta E_B^2|_{\text{loc}} + \Delta E_B^2|_{\text{ent}}$, where

$$\Delta E_B^2|_{\text{loc}} \equiv \sum_i [\text{Tr}[h_i^2 \rho_B] - \text{Tr}[h_i \rho_B]^2], \quad (22)$$

$$\Delta E_B^2|_{\text{ent}} \equiv \sum_{i \neq j} [\text{Tr}[h_i h_j \rho_B] - \text{Tr}[h_i \rho_B] \text{Tr}[h_j \rho_B]]. \quad (23)$$

The first quantity $\Delta E_B^2|_{\text{loc}}$ in Eq. (22), a sum of local terms, scales linearly with N by construction. However, $\Delta E_B^2|_{\text{ent}}$, whose explicit form can be immediately linked to correlations between sites i and j , may display a superlinear scaling with N if correlations between different battery units are developed. With this approach, Julià-Farré *et al.* (2020) obtained a bound on the instantaneous power $P(t)$,

$$P(t) \leq \sqrt{\Delta E_B^2(t) I_E(t)}, \quad (24)$$

whose geometric interpretation is illustrated in Fig. 3, as well as a similar bound on the average power $\langle P \rangle_\tau \leq \sqrt{\langle \Delta E_B^2 \rangle_\tau \langle I_E \rangle_\tau}$ (Julià-Farré *et al.*, 2020).

As detailed in Sec. III.B.3, Julià-Farré *et al.* (2020) used this method to confirm that the advantage discussed by Binder *et al.* (2015b) and Campaioli *et al.* (2017) is quantum since it stems from nonlocal correlations, while that of the Dicke battery (Sec. III.B) is collective since it stems from a higher speed in the energy eigenspace that is characterized by more extensive Fisher information I_E . The importance of the bound on power discussed by Julià-Farré *et al.* (2020) is striking since it enables the discrimination between a collective advantage in power emerging from the Fisher information

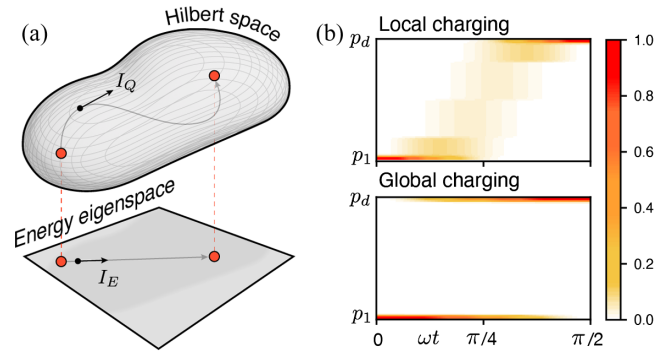


FIG. 3. (a) The speed I_Q of quantum dynamics in the Hilbert space and the speed $I_E \leq I_Q$ in the energy eigenspace of the battery Hamiltonian are related to the quantum Fisher information. The instantaneous charging power is bounded by I_E as in Eq. (24). (b) Dynamics of the energy levels p_k associated with the internal Hamiltonian $H^{(N)}$ of Eq. (8) during local ($H_1^{(N)}$) and global ($H_N^{(N)}$) charging, where ω is the associated charging frequency. The global charging scheme takes a shortcut in the Hilbert space by driving the battery through the maximally entangled state $|\psi\rangle \propto |G\rangle + |E\rangle$. Adapted from Julià-Farré *et al.*, 2020.

and a genuine quantum advantage due to quantum correlations between battery cells. Note also that their approach does not require the definition of an analog classical Hamiltonian \mathcal{H}_B . Power bounds have been generalized to the case of open quantum batteries (Zakavati, Tabesh, and Salimi, 2021) and should be an object of further study.

III. MODELS OF MANY-BODY BATTERIES

At the microscopic level, matter is granular as it can be described in terms of a collection of N elementary units, such as atoms or molecules. In many cases, the behavior of a macroscopic system can be accurately described by assuming that these units behave independently, leading to intensive quantities (such as pressure) that do not depend on the size of the system or to extensive quantities (such as energy or volume) that scale linearly with the number of constituent units N . However, in some cases interactions between the elementary units can give rise to collective effects that cannot be explained by the properties of a single unit. These collective effects can result in macroscopic quantities showing a superextensive scaling N^α with $\alpha > 1$.

An example of paramount importance is provided by the Dicke model (Dicke, 1954), where an ensemble of N atoms collectively radiates with a superextensive intensity that scales as N^2 , i.e., is enhanced by a factor N with respect to ordinary fluorescence. In the latter case, atoms emit independently. In the former, synchronization of the electrical dipoles of the atoms occurs, leading to an enhanced emission that has been named superradiance (Gross and Haroche, 1982; Haroche, 2013).

Superradiant emission has been measured in a plethora of different systems, such as Rydberg atoms in a cavity (Kaluzny *et al.*, 1983) and color centers in diamond (Angerer *et al.*, 2018). The concept of superabsorption (Higgins *et al.*, 2014), where collective effects are used to speed up energy absorption, has also been proposed based on the time-reversal symmetry of the superradiant dynamics of an ensemble of emitters interacting with electromagnetic radiation (Yang *et al.*, 2021).

Ferraro *et al.* (2018) proposed a model of a battery that could be engineered in a solid-state device. The quantum many-body model comprises N TLSs coupled to the same mode of an electromagnetic field. For these reasons, the battery was termed the Dicke quantum battery. There were three reasons for proposing such a model: (i) the fact that the N TLSs were coupled to the same cavity mode effectively provided a way to couple all the TLSs together during the nonequilibrium dynamics, (ii) the superradiant collective effects displayed by the previously discussed Dicke model were thought to be useful in determining an advantage in the charging process, and (iii) as we see in Sec. VI, Dicke models can be experimentally realized in a variety of ways. Quach *et al.* (2022) observed collective effects in the charging process of a superabsorber. In Secs. III.A–III.D, we review the charging properties of a variety of many-body battery models.

A. Charging protocols and figure of merits

We begin with a presentation of a framework for describing the charging process. The battery is a system B , described by a

Hamiltonian $H_B^{(0)}$ consisting of N identical units. It is often assumed that the battery Hamiltonian is the sum of N local Hamiltonians: $H_B^{(0)} = \sum_{i=1}^N h_i^{(B)}$. The battery is initially prepared in the ground state, and energy is injected into the battery through a charging protocol with a time duration τ . After the protocol, the energy stored in the battery $W(\tau)$ is given by Eq. (3), i.e., $W(\tau) = \text{Tr}[H_B^{(0)}\rho_B(\tau)]$, where $\rho_B(\tau)$ is the state of the battery at the time τ and the second term in Eq. (3) vanishes as the ground-state energy is fixed to zero.

1. Direct charging protocol

In a *direct charging protocol*, the Hamiltonian of the battery is externally changed by suddenly switching on an interaction Hamiltonian $H_B^{(1)}$ for a charging time τ while switching off $H_B^{(0)}$ (Binder *et al.*, 2015b; Campaioli *et al.*, 2017; Le *et al.*, 2018; Rossini, Andolina, and Polini, 2019; Rosa *et al.*, 2020; Rossini *et al.*, 2020), as depicted in Fig. 4(a). The battery dynamics is therefore dictated by the following time-dependent Hamiltonian:

$$H_B(t) = H_B^{(0)} + \lambda(t)(H_B^{(1)} - H_B^{(0)}), \quad (25)$$

where $\lambda(t)$ is a classical parameter representing an external control. The term $H_B^{(1)}$ is referred to as the charging Hamiltonian, and $H_B^{(0)}$ is the battery Hamiltonian. In this case, all energy is injected in the battery by the external classical control. For simplicity, we have assumed that the control is a step function that is equal to 1 during the charging time $t \in [0, \tau]$ and zero otherwise.

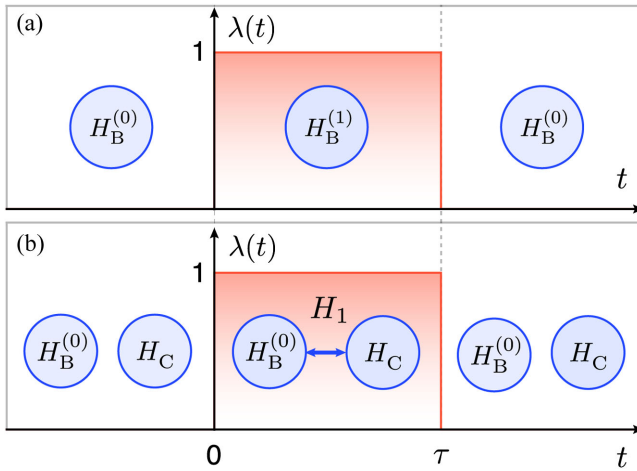


FIG. 4. (a) In a time-dependent direct charging protocol, the Hamiltonian of the battery is externally changed by suddenly quenching an interaction Hamiltonian $H_B^{(1)}$ for a finite amount of time τ , while the battery Hamiltonian $H_B^{(0)}$ is turned off during the charging process. (b) In a charger-mediated protocol, a “charger” C initially containing some input energy transfers energy to the battery B. The charging process is enabled by an interaction Hamiltonian H_1 that couples the charger and the battery for a finite amount of time τ .

2. Charger-mediated protocol

In the *charger-mediated protocol* (Andolina *et al.*, 2018; Ferraro *et al.*, 2018; Andolina, Keck, Mari, Campisi *et al.*, 2019; Farina *et al.*, 2019; Crescente *et al.*, 2020a; Delmonte *et al.*, 2021), an auxiliary system referred to as the charger C is introduced. Initially, the charger contains a certain amount of energy, which is intended to be transferred to the battery B. The charging process occurs due to an interaction between the charger and the battery that lasts a charging time τ , as depicted in Fig. 4(b). Thus, the global Hamiltonian of the composite CB system is

$$H(t) = H_0 + \lambda(t)H_1, \quad (26)$$

$$H_0 = H_C + H_B^{(0)}, \quad (27)$$

where H_C is the charging Hamiltonian, H_1 is the interaction Hamiltonian, and $\lambda(t)$ is an external control. In this protocol, the composite system CB [described by the composite state $\rho_{CB}(t)$] can exchange work with the environment through the classical control, leading to some energy ambiguity.

The external control $\lambda(t)$ modulates the interaction between the charger and the battery. It may introduce an energy cost $W_{sw}(\tau)$ (Andolina *et al.*, 2018) at switching times, specifically when the external control is switched on at $t = 0$ and switched off at $t = \tau$. Note that in such a case the total system energy $E(t) = \text{Tr}[H(t)\rho_{CB}(t)]$ remains constant except at the switching times (0 and τ). The energy cost can be thus expressed as $W_{sw}(\tau) \equiv \lim_{\epsilon \rightarrow 0} \{[E(\tau + \epsilon) - E(\tau - \epsilon)] + [E(\epsilon) - E(-\epsilon)]\}$. By ensuring that H_1 only exchanges well-defined excitations of the bare Hamiltonian H_0 , i.e., $[H_0, H_1] = 0$, the energy transfer from the charger to the battery becomes unambiguous as the energy cost vanishes: $W_{sw}(\tau) = 0$. If the interactions are noncommuting, i.e., $[H_0, H_1] \neq 0$, the final energy of the quantum battery is partially supplied by the modulation of $\lambda(t)$, as shown by Andolina *et al.* (2018) and Chiara *et al.* (2018). This introduces an element of arbitrariness in the charging protocol given that the energy transfer does not exclusively occur between the charger and the battery (Ferraro *et al.*, 2018).

B. Charging properties of the Dicke quantum battery

1. The Dicke battery

We now discuss a quantum battery based on the Dicke model (Dicke, 1954). The model describes the collective interaction of an ensemble of N TLS atoms with a single mode of the cavity field,

$$H_{\text{Dicke}} = \omega_c \hat{a}^\dagger \hat{a} + \omega_0 \sum_{i=1}^N \hat{\sigma}_i^z + g \sum_{i=1}^N \hat{\sigma}_i^x (\hat{a}^\dagger + \hat{a}). \quad (28)$$

In Eq. (28) \hat{a} (\hat{a}^\dagger) annihilates (creates) a cavity photon with a frequency ω_c , ω_0 is the resonant frequency of a TLS $\hat{\sigma}_i^\alpha$, with $\alpha = x, y, z$ the components of the Pauli operators $\hat{\sigma}_i^\alpha$ of the i th TLS, and g is the TLS-cavity coupling parameter. Cavities are typically composed of two mirrors that reflect light back and forth, creating a standing wave of electromagnetic radiation

(Haroche, 2013), whose frequencies are determined by the cavity's geometry. In this context, the single-mode approximation is typically employed since one of the cavity modes is designed to be resonant with the atomic transition frequency. This resonant mode dominantly interacts with the atoms, while the interaction with off-resonant modes is negligible. Note that when deriving the Dicke model from a microscopic underlying model, the light-matter coupling g is found to scale as $1/\sqrt{V}$, where V is the volume of the cavity. This scaling has significant implications that are discussed in Sec. III.B.4.

The Dicke model represents a situation where all atoms are collectively coupled to the same cavity mode. Thus, tracing out this cavity mode results in a scenario where all the TLSs interact with each other, i.e., the so-called all-to-all interaction (corresponding to a participation number $m = N$; see Sec. II.C.3). Ferraro *et al.* (2018) proposed the use of the Dicke model for a quantum battery due to its experimental feasibility and relation with superradiant emission.

In the Dicke battery, the charging is performed via a charger-mediated protocol, where the cavity acts as a charger while the TLSs are seen as the battery. During the charging, one aims to transfer the energy of the cavity to the TLSs. The quantum dynamics of this Dicke charging protocol is described by the following Hamiltonian terms:

$$H_C = \omega_c \hat{a}^\dagger \hat{a}, \quad (29)$$

$$H_B^{(0)} = \frac{\omega_0}{2} \sum_{i=1}^N (\hat{\sigma}_i^z + 1), \quad (30)$$

$$H_1 = g \sum_{i=1}^N \hat{\sigma}_i^x (\hat{a}^\dagger + \hat{a}), \quad (31)$$

to be compared with the generic charger-mediated protocol defined by Eq. (26). During the charging dynamics where the time t is in the interval $[0, \tau]$, the evolution of the state is dictated by the Dicke Hamiltonian in Eq. (28). To begin, the system is initialized in the state

$$|\psi^{(n)}(0)\rangle = |n\rangle \otimes |G\rangle, \quad (32)$$

where $|n\rangle$ is a Fock state of n photons in the cavity and $|G\rangle = \otimes^N |g\rangle$, with $|g\rangle$ the ground state of each TLS. Since the goal is to fully charge the TLSs, it is convenient to inject into the cavity a number n of photons that is at least equal to N . Ferraro *et al.* (2018) took $n = N$ and enforced the resonant condition $\omega_0 = \omega_c$ to favor energy transfer. Finally, Ferraro *et al.* (2018) chose the charging time to be the optimal charging time $\tilde{\tau}$ that maximizes the average power, i.e., $\langle P \rangle_{\tilde{\tau}} = \max_{\tau} [\langle P \rangle_{\tau}]$.

2. Parallel versus collective charging

To quantify whether charging the TLSs via the collective coupling H_1 in Eq. (31) yields an advantage, Ferraro *et al.* (2018) compared the maximum charging power $\langle P_{\#} \rangle_{\tilde{\tau}}$ that can be obtained in the *collective charging case*, i.e., via the Dicke interaction term in Eq. (31), with the maximum charging power $\langle P_{\parallel} \rangle_{\tilde{\tau}}$ that can be achieved through ‘‘parallel charging.’’

In the latter charging scheme, N identical systems, each comprising a single TLS interacting with its own cavity containing a single photon ($n = 1$), are considered. Each system is a Rabi battery, i.e., a battery described using the Rabi model (Braak, 2011),

$$H_{\text{Rabi}} = \omega_c \hat{a}^\dagger \hat{a} + \omega_0 \hat{\sigma}^z + g \hat{\sigma}^x (\hat{a}^\dagger + \hat{a}). \quad (33)$$

Parallel and collective charging protocols are illustrated in Figs. 5(a) and 5(b), respectively.

Ferraro *et al.* (2018) showed that, in the limit $N \gg 1$,

$$\frac{\langle P_{\#} \rangle_{\tilde{\tau}}}{\langle P_{\parallel} \rangle_{\tilde{\tau}}} \sim \sqrt{N}. \quad (34)$$

This advantage stems from the superextensive scaling of the collective power $\langle P_{\#} \rangle_{\tilde{\tau}} \sim N^{3/2}$ and from the extensive scaling of the parallel charging power $\langle P_{\parallel} \rangle_{\tilde{\tau}} \sim N$, as shown in Fig. 5(c). Note that the quantity $\langle P_{\parallel} \rangle_{\tilde{\tau}}$ scales extensively with N because, by construction, the parallel charging scheme is free of collective behavior. Since in both cases the energy $\langle H_B^{(0)} \rangle_{\tilde{\tau}}$ of the battery scales extensively with the number of

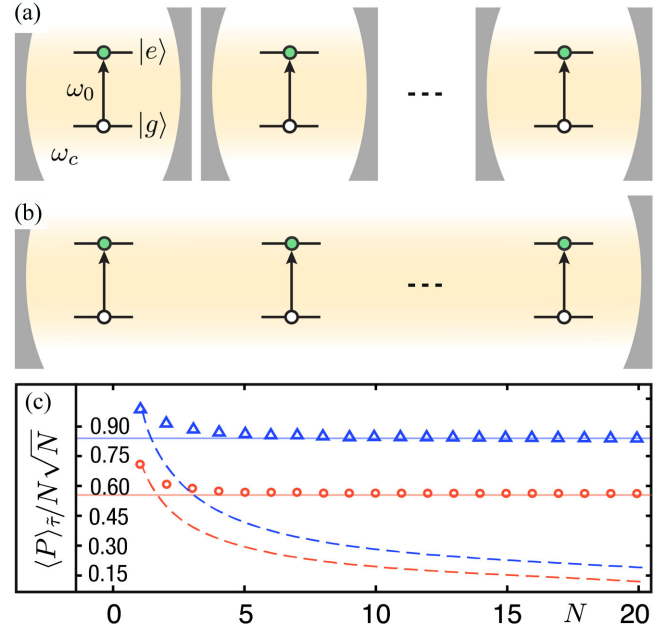


FIG. 5. (a) Parallel charging protocol for an array of identical Rabi batteries. The single battery unit consists of a two-level system with transition energy ω_0 between the ground state $|g\rangle$ and excited state $|e\rangle$. Each two-level system is coupled to its own cavity hosting a single mode with frequency ω_c . In the corresponding collective charging protocol, a Dicke quantum battery is composed by N two-level systems coupled to the same photonic mode. (c) The maximum average power $\langle P \rangle_{\tilde{\tau}}$ (divided by the factor $N\sqrt{N}$) is plotted as a function of the number N of qubits. Solid (dashed) lines refer to the collective (parallel) protocol. The collective advantage manifests as a saturation to a constant (solid lines) for $N \gg 1$ of the collective-case maximum power divided by $N\sqrt{N}$. The red lines correspond to the weak-coupling regime (i.e., $g/\omega_0 = 0.05$), while the blue lines correspond to the strong-coupling regime (i.e., $g/\omega_0 = 0.5$). Adapted from Ferraro *et al.*, 2018.

battery units N , this advantage corresponds to a speedup in the optimal charging time $\bar{\tau} \sim 1/\sqrt{N}$.

The Dicke battery therefore displays a collective speedup in the charging time, outperforming the parallel charging protocol by a \sqrt{N} factor. The Dicke battery model has seen extensive exploration and diverse generalizations. For instance, the charging process has been optimized in the simplified case where the semiclassical limit is taken (Zhang *et al.*, 2019; Crescente *et al.*, 2020a). Researchers have also studied whether this speedup has a quantum or collective origin (Andolina, Keck, Mari, Giovannetti, and Polini, 2019; Julià-Farré *et al.*, 2020) and a two-photon version of the model (Crescente *et al.*, 2020b, 2022; Delmonte *et al.*, 2021), where an atomic excitation can be converted into two resonant photons, and vice versa. Other aspects of the Dicke model, such as the task of energy extraction, have also been examined (Andolina, Keck, Mari, Campisi *et al.*, 2019). In the remainder of this section, we review these issues in more detail.

3. Origin of the charging advantage

Using the arguments presented in Secs. II.C.2 and II.C.4, we now show that the Dicke battery's collective speedup has a many-body collective origin rather than a genuine quantum one. A first hint that the Dicke battery's charging speedup is not related to entanglement was given by Andolina *et al.* (2018), who studied a simplified version of the Rabi battery. It consisted of a single TLS described by the Hamiltonian $H_B^{(0)} = \omega_0(\hat{\sigma}^z + \mathbb{1})/2$, which is charged by a cavity mode initialized in a Fock state with n photons. The simplification with respect to the Rabi model lies in the fact that the interaction Hamiltonian H_1 chosen by Andolina *et al.* (2018) contained only rotating terms, i.e., $H_1 = g(\hat{\sigma}^- \hat{a}^\dagger + \hat{\sigma}^+ \hat{a})$, where $\hat{\sigma}^+$ ($\hat{\sigma}^-$) is the Pauli creation (annihilation) operator. In this case, the time $\bar{\tau}$ required to reach the maximum energy can be calculated analytically, and it was found to scale as $\bar{\tau} \sim 1/\sqrt{n}$. This simple example demonstrates that it is possible to speed up the charging process by a factor $1/\sqrt{n}$ for a single TLS by initially placing n photons in the cavity. Only one excitation is transferred from the charger to the quantum battery in this protocol, with the remaining $n - 1$ excitations acting as a ‘‘catalytic resource’’ to increase the speed of the process. Since there is only one battery unit in this protocol, this example also illustrates that entanglement between different units is not necessary to achieve a charging speedup. Along these lines, Zhang and Blaauboer (2023) analyzed the Dicke battery without assuming $n = N$, showing that the charging time scales as $\bar{\tau} \sim 1/\sqrt{n}$ in the limit $n \gg N$.

Another hint came from the analysis of a Dicke battery in the case in which the cavity is initialized in a coherent state with an average number of photons N . In this case, the charging dynamics leads to low entanglement between the charger and the battery (Andolina, Keck, Mari, Campisi *et al.*, 2019). Notwithstanding, the Dicke battery still exhibits a collective speedup $\bar{\tau} \sim 1/\sqrt{N}$.

Finally, Andolina, Keck, Mari, Giovannetti, and Polini (2019) questioned the quantum origin of the charging speedup of a series of many-body batteries, including the Dicke one. Their study was based on a comparison between

quantum-mechanical many-body batteries and the corresponding classical models. The correspondence was obtained at the Hamiltonian level by replacing quantum commutators with classical Poisson brackets, as discussed in Sec. II.C.4. Here we focus specifically on the Dicke battery. Using the fact that the Dicke model has a well established classical analog (de Aguiar *et al.*, 1992; Rodriguez, Chilingaryan, and Rodríguez-Lara, 2018; Chávez-Carlos *et al.*, 2019), one can easily construct a classical Dicke battery that is described by the following Hamiltonian:

$$\mathcal{H}_B^{(0)} = N\omega_0 \frac{1 + \cos(\theta)}{2}. \quad (35)$$

The charger is described by a classical harmonic oscillator

$$\mathcal{H}_C = \frac{\omega_0}{2}(p_a^2 + q_a^2). \quad (36)$$

Finally, charging occurs via the following classical interaction Hamiltonian:

$$\mathcal{H}_1 = g\sqrt{2}Nq_a \sin(\theta) \cos(\phi). \quad (37)$$

In Eq. (36) (p_a, q_a) and $((N/2)\cos(\theta), \phi)$ are conjugate variables (Chávez-Carlos *et al.*, 2019). The classical protocol in Eqs. (35)–(37) has to be interpreted as a charger-mediated protocol, dictated by a classical Hamiltonian $\mathcal{H}(t) = \mathcal{H}_B^{(0)} + \mathcal{H}_C + \lambda(t)\mathcal{H}_1$.

Andolina, Keck, Mari, Giovannetti, and Polini (2019) calculated the charging power of the classical Dicke Hamiltonian, finding that the collective advantage Γ_c introduced in Eq. (21) scales like \sqrt{N} . This should be contrasted with the quantum collective advantage Γ_q of the Dicke battery [see Eq. (29)], i.e., $\Gamma_q \sim \sqrt{N}$. Hence, in the case of a Dicke battery the ratio R defined in Eq. (21) was found not to scale with N . For Dicke batteries, R depends on the value of the coupling constant g that controls the interaction between the charger and the battery itself. This analysis clarified that no quantum advantage R scaling with N can be found in the charging dynamics of the Dicke battery. Similar results were found for other many-body battery models.

4. Charging advantage in the thermodynamic limit

As discussed in Sec. II.C.4, Julià-Farré *et al.* (2020) derived a bound for the average charging power $\langle P \rangle_\tau \leq \sqrt{\langle \Delta E_B^2 \rangle_\tau \langle I_E \rangle_\tau}$, which allows one to distinguish a genuine entanglement-induced speedup (arising from the first term, the variance of the battery Hamiltonian $\langle \Delta E_B^2 \rangle_\tau$) from a collective many-body speedup (stemming from the second term, the quantum Fisher information $\langle I_E \rangle_\tau$). This bound was employed to study the charging dynamics of the Dicke battery introduced in Eqs. (29)–(31); τ was fixed to maximize the energy stored in the battery, i.e., $\tau = \bar{\tau}$. However, a different normalization with respect to that in Eq. (31) was used for the interaction Hamiltonian H_1 upon making the replacement

$$g \rightarrow g_{\text{TD}} \equiv \frac{g}{\sqrt{N}} \quad (38)$$

in Eq. (31).

This normalization is used when analyzing the phase diagram of the Dicke model, as described by Hepp and Lieb (1973) and Wang and Hioe (1973), and guarantees that the total energy and energy fluctuations of the Dicke model will exhibit a well-defined, extensive behavior in the thermodynamic limit ($N \rightarrow \infty$ and $V \rightarrow \infty$ while maintaining a constant ratio N/V). Here V represents the volume of the cavity, which is assumed to scale linearly with the number of TLSs N to ensure a constant density of TLSs N/V .

Julià-Farré *et al.* (2020) analytically derived a bound on the scaling of the quantum Fisher information $I_E(t)$, thereby obtaining $\sqrt{I_E(t)} \lesssim \sqrt{N}$. In the weak-coupling $g \ll \omega_0$ limit, the variance of the battery Hamiltonian $\sqrt{\langle \Delta E_B^2 \rangle_\tau}$ (see also Sec. II.C.4) scales as $\sim N^{0.44}$. The bound $\sqrt{\langle \Delta E_B^2 \rangle_\tau \langle I_E \rangle_\tau}$ was therefore found to scale sublinearly with N , i.e., $\sqrt{\langle \Delta E_B^2 \rangle_\tau \langle I_E \rangle_\tau} \lesssim N^{0.94}$. On the contrary, in the strong-coupling $g = \omega_0/2$ regime, the term $\sqrt{\langle \Delta E_B^2 \rangle_\tau}$ was found to scale as $\sim N^{0.92}$, yielding $\sqrt{\langle \Delta E_B^2 \rangle_\tau \langle I_E \rangle_\tau} \lesssim N^{1.42}$. Julià-Farré *et al.* (2020) also found that in the strong-coupling regime the average power scales extensively as $\langle P \rangle_\tau \sim N$, despite the quantum enhancement in $\sqrt{\langle \Delta E_B^2 \rangle_\tau}$. This is because in this case the bound derived is significantly looser and far from being saturated, with $\langle P \rangle_\tau \ll \sqrt{\langle \Delta E_B^2 \rangle_\tau \langle I_E \rangle_\tau}$. This explains why, in the case of the Dicke battery, the bound fails to accurately predict the scaling behavior of the charging power.

We now observe that if the normalization in Eq. (31) is adopted, as it was by Ferraro *et al.* (2018), one finds that $\sqrt{\langle I_E \rangle_\tau}$ scales linearly in N even if $\sqrt{\langle \Delta E_B^2 \rangle_\tau} \sim \sqrt{N}$, and the bound on power $\langle P \rangle_\tau$ scales superextensively as $N\sqrt{N}$ without the requirement of any quantum superextensive scaling in $\sqrt{\langle \Delta E_B^2 \rangle_\tau}$. This means that to accelerate the charging process entanglement generation is not essential in this case, as \sqrt{N} even in the absence of system correlations; see Eq. (22). In agreement with the findings of Andolina, Keck, Mari, Giovannetti, and Polini (2019), Julià-Farré *et al.* (2020) concluded that the Dicke battery model does not exhibit a genuine quantum advantage.

However, while the replacement $g \rightarrow g/\sqrt{N}$ is necessary when considering a thermodynamic limit with a fixed density N/V , there are instances where $N \gg 1$ is large but finite and there is no need to scale the cavity length to accommodate more battery units. When derived from fundamental principles, the light-matter coupling strength scales as $g \sim 1/\sqrt{V}$, where V is the cavity volume. Hence, there are experimental platforms where there is no need to adopt the normalization in Eq. (38), as the cavity volume V can be kept fixed, while the number of atoms N is varied. For instance, cavity quantum electrodynamics experiments that study superradiance are performed in this limit even if the number of atoms is large ($N \sim 10^3$) (Haroche, 2013). The capacity to accommodate numerous atoms in a single fixed cavity stems from the significant size disparity between a typical cavity (approximately a few centimeters, or around 1 cm for microwave cavities) and the effective size of an atom (a few micrometers for Rydberg atoms). Hence, to describe these experiments the normalization of Eq. (38) is not adopted. As Andolina, Keck, Mari, Giovannetti, and Polini (2019) discussed, whether one

uses Eq. (29) with or without the renormalization $g \rightarrow g/\sqrt{N}$ ultimately depends on the specific experimental setup.

5. Variations of the Dicke batteries

Owing to the success of the Dicke battery model, several variations of it were subsequently proposed. Recent studies on trapped-ion (Felicetti *et al.*, 2015) and superconducting-flux-qubit setups (Felicetti *et al.*, 2018) showed the potential to suppress the dipole contribution, which is linear in the photon coupling [Eq. (31)], thereby enhancing the two-photon coupling. If the TLSs of a Dicke battery are set to be resonant with twice the cavity frequency ($\omega_0 = 2\omega_c$), their dynamics is dominated by two-photon processes that are described as the so-called two-photon Dicke model. This model presents an interesting phase diagram with two quantum criticalities: (i) the superradiant phase transition (Garbe *et al.*, 2017) and (ii) a spectral collapse (Garbe *et al.*, 2020). In this context, Crescente *et al.* (2020b) focused on two-photon Dicke quantum batteries in which the interaction Hamiltonian in Eq. (29) was replaced by the following one:

$$H_1 = g_{2\text{ph}} \sum_{i=1}^N \hat{\sigma}_i^x [(\hat{a}^\dagger)^2 + (\hat{a})^2], \quad (39)$$

where $g_{2\text{ph}}$ is the coupling strength for the two-photon processes. Crescente *et al.* (2020b) found that the maximum charging power scaled quadratically in N , $\langle P \rangle_\tau \sim N^2$, which is \sqrt{N} times faster than the conventional Dicke battery. However, they noted that if consistency with the thermodynamic limit (discussed in Sec. III.B.3) is enforced, the two-photon coupling needs to be rescaled as $g_{2\text{ph}} \rightarrow g_{2\text{ph}}/N$, which exactly cancels the superextensive scaling of the power, yielding $\langle P \rangle_\tau \sim 1$. Additionally, the scaling of energy fluctuations (Crescente *et al.*, 2020b), the extractable work, and the dependence upon the initial photonic state (Delmonte *et al.*, 2021) were also studied in this model. Recently Gemme *et al.* (2023) studied a case in which a Dicke quantum battery was driven with off-resonant pulses via an exchange of virtual photons.

The Dicke model is a widely used tool to describe atoms interacting with a cavity. In some physical situations, however, it may require extensions. For example, in a Bose-Einstein condensate coupled to an optical cavity, direct dipole-dipole interactions between different atoms need to be considered (Baumann *et al.*, 2010; Rodriguez, Chilingaryan, and Rodríguez-Lara, 2018). Dou *et al.* (2022) considered an extended Dicke model that includes an interatomic interaction term in addition to the atom-photon Dicke coupling Hamiltonian in Eq. (31). This model was found to exhibit faster battery charging in the strong-coupling regime, with a maximum power scaling of $\langle P \rangle_\tau \sim N^{1.88}$. Not surprisingly, in the weak-coupling regime the power was found to scale as $\sim N^{1.5}$ as in the conventional Dicke model. Another variation of the Dicke model was studied by Dou, Zhou, and Sun (2022) who examined the charging dynamics of a Heisenberg spin-chain battery (see Sec. III.C.1) and found that the maximum power scaling was at most $\langle P \rangle_\tau \sim N^{0.75}$. A superconducting implementation of an extended Dicke battery was recently

proposed by [Dou and Yang \(2023\)](#). However, by coupling the spin-chain battery to a common cavity field, it was possible to enhance the maximum power scaling to $\sim N^2$ ([Dou, Zhou, and Sun, 2022](#)). The extended Dicke model was also studied by [Zhao, Dou, and Zhao \(2022\)](#), while [Yang, Yang, and Dou \(2023\)](#) recently studied a three-level version of the Dicke battery.

C. Charging properties of other many-body batteries

1. Spin-chain and spin-network batteries

A spin chain is a one-dimensional array of TLSs that interact with each other. These theoretical models have been widely studied in the field of condensed matter physics; they are closely related to the study of magnetism ([Auerbach, 1994](#)) and have also been applied to quantum devices, communication, and computation ([Zueco *et al.*, 2009](#)). [Le *et al.* \(2018\)](#) proposed a spin-chain model of a many-body quantum battery in which energy is injected via the direct charging protocol introduced in Eq. (25), where the battery Hamiltonian is

$$H_B^{(0)} = B \sum_{i=1}^N \hat{\sigma}_i^z - \sum_{i<j} g_{ij} [\hat{\sigma}_i^z \hat{\sigma}_j^z + \alpha (\hat{\sigma}_i^x \hat{\sigma}_j^x + \hat{\sigma}_i^y \hat{\sigma}_j^y)] \quad (40)$$

and the charging Hamiltonian is $H_B^{(1)} = \omega \sum_{i=1}^N \hat{\sigma}_i^x$. In Eq. (40) B is the strength of an external Zeeman field and g_{ij} is the interaction strength. The anisotropy parameter α can be tuned to recover Ising ($\alpha = 0$), XXZ ($0 < \alpha < 1$), and XXX Heisenberg models ($\alpha = 1$) ([Le *et al.*, 2018](#)). Additionally, a transverse magnetic field parametrized by ω is used to charge the system. Either nearest-neighbor $g_{ij} = g\delta_{i,j}$ or long-range $g_{ij} = g/|i-j|^p$ interactions, with $p > 0$, are considered.

Unlike customary battery models, energy can be stored in the interactions between the different spins, as the battery Hamiltonian is not a sum of local independent terms. This implies that the eigenstates of the internal Hamiltonian $H_B^{(0)}$ can be entangled if the coupling strength g_{ij} is nonvanishing due to the presence of two-body interactions between the spins. In reference to the discussion in Sec. II.C.3, the N battery units are interacting via a $k = \text{two-body}$ interaction term with an arbitrarily long range, corresponding to a participation number m that scales with the system size as $m = N$. This comparison, in light of Eq. (19), implies that the power is bounded to scale quadratically with size, i.e., $\langle P \rangle_{\bar{\tau}} \sim N^2$ in the long-range scenario.

In addition, the role of the anisotropy α and the interaction range was discussed by [Le *et al.* \(2018\)](#). The isotropic coupling of the XXX Heisenberg model ($\alpha = 1$) resulted in the independent charging of each spin. This phenomenon occurs even in the presence of interactions, because for $\alpha = 1$ the battery Hamiltonian $H_B^{(1)}$ commutes with these interactions due to rotational invariance of the model. Consequently, the XXX model exhibits an extensive maximum power $\langle P \rangle_{\bar{\tau}} \sim N$. Conversely, the full anisotropy of the XXZ model, i.e., $\alpha = -1$, leads to much higher power than in the independent case.

In the weak-coupling $\sum_{i<j} g_{ij} \ll N\omega$ regime, the scaling of the maximum power is analyzed. In particular, in the case of nearest-neighbor interactions, the power is extensive in N . When the coupling strength decays algebraically as $1/|i-j|$ ($p = 1$), where i and j denote the lattice size along the chain, the charging power grows superextensively as $\langle P \rangle_{\bar{\tau}} \sim N \log(N)$. Finally, for a ‘‘uniform’’ $p = 0$ interaction strength, a superextensive power $\langle P \rangle_{\bar{\tau}} \sim N^2$ is found.

[Le *et al.* \(2018\)](#) discussed a strategy to implement the global entangling Hamiltonian in Eq. (17) proposed by [Binder *et al.* \(2015b\)](#) and [Campaioli *et al.* \(2017\)](#). In the limit of strong nearest-neighbor attractive interactions ($g \gg \omega$), it is possible to write an effective global entangling Hamiltonian with a $k = N$ -body interaction. However, this effective interaction scales as $\omega(\omega/g)^N$, and since it has been obtained in the perturbative regime $g \gg \omega$ exponentially vanishes in the limit of large N . For this reason, the power deposited in the battery actually worsens when the spins traverse the correlated shortcut suggested by [Binder *et al.* \(2015a\)](#) and vanishes in the $N \rightarrow \infty$ limit. The study of spin-chain batteries has been further extended to disordered models; see [Rossini, Andolina, and Polini \(2019\)](#) and [Ghosh, Chanda, and Sende \(2020\)](#). Additionally, separate investigations have focused on charging spin chains through the use of a cavity mode ([Dou, Zhou, and Sun, 2022](#)) or another spin system ([Yang *et al.*, 2020](#); [Huangfu and Jing, 2021](#); [Liu *et al.*, 2021](#); [Lu *et al.*, 2021](#); [Peng *et al.*, 2021](#); [Qi and Jing, 2021](#); [Zhao, Dou, and Zhao, 2021](#); [Arjmandi, Mohammadi, and Santos, 2022](#); [Barra, Hovhannisyanyan, and Imperato, 2022](#); [Gao *et al.*, 2022](#); [Ghosh and De, 2022](#); [Konar, Lakkaraju *et al.*, 2022](#); [Yao and Shao, 2022](#); [Crescente *et al.*, 2023](#); [Rodríguez *et al.*, 2023](#); [Guo, Yang, and Dou, 2024](#)).

2. SYK quantum batteries

Motivated by the discussions reported in Secs. II.C.4 and III.B.3, [Rossini *et al.* \(2020\)](#) proposed a model for a many-body battery that unequivocally presents a genuine quantum advantage [certified using the bound of [Julià-Farré *et al.* \(2020\)](#)].

This implementation relies on the SYK model ([Sachdev and Ye, 1993](#); [Kitaev, 2015](#)). The SYK model describes quantum matter defying the Landau paradigm of normal Fermi liquids in that it displays no quasiparticles. It has garnered a great deal of attention in recent years due to its unique properties, which include fast scrambling ([Maldacena and Stanford, 2016](#)), nonzero entropy density at vanishing temperature ([Georges, Parcollet, and Sachdev, 2001](#)) and volume-law entanglement entropy in all its eigenstates ([Liu, Chen, and Balents, 2018](#)), and it is holographically connected to the dynamics of the two-dimensional anti-de Sitter horizon of a quantum black hole ([Kitaev, 2015](#)).

The SYK battery introduced by [Rossini *et al.* \(2020\)](#), which is illustrated in Fig. 6(a), is charged via a direct charging protocol, as in Eq. (25). The internal battery Hamiltonian $H_B^{(0)}$ is a sum of local terms given by

$$H_B^{(0)} = \sum_{i=0}^N \omega_0 \sigma_i^y, \quad (41)$$

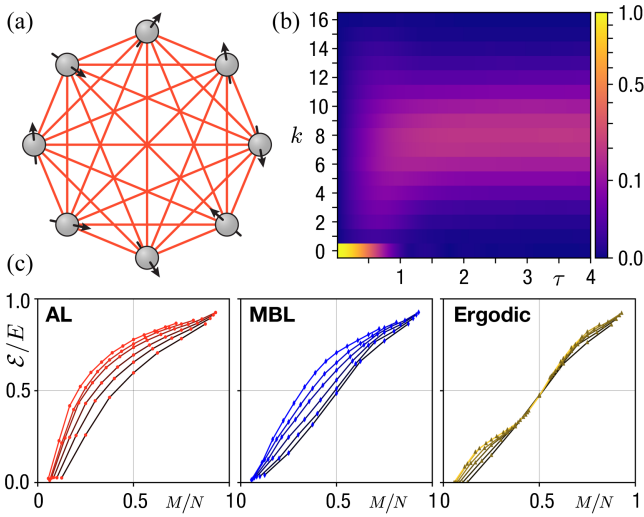


FIG. 6. (a) Sketch of the SYK model (Sachdev and Ye, 1993; Kitaev, 2015) for randomly interacting fermions with all-to-all interactions. (b) Dynamics of the populations p_k of the k th energy level associated with the battery Hamiltonian $H_B^{(0)}$; cf. Fig. 3(b). The charging Hamiltonian consists of the cSYK Hamiltonian $H_B^{(1)}$ of Eq. (48). This global charging scheme takes a shortcut in the Hilbert space by driving the battery through maximally entangled states. This can be seen in the short-time behavior of the populations. In this regime, the populations do not propagate locally in the Hilbert space, as in the case of global charging; see Fig. 3(b). (c) Fraction of useful energy \mathcal{E}/E as a function of the fraction M/N at a fixed time τ . This quantity can be used to discriminate whether the system is in an Anderson localized (AL), many-body localized (MBL), or ergodic phase.

while charging is performed via the complex SYK (cSYK) Hamiltonian

$$H_B^{(1)} = \sum_{i,j,k,l=1}^N J_{i,j,k,l} \hat{c}_i^\dagger \hat{c}_j^\dagger \hat{c}_k \hat{c}_l. \quad (42)$$

In Eq. (42) \hat{c}_j^\dagger (\hat{c}_j) is a spinless fermionic creation (annihilation) operator. This has to be understood in its spin-1/2 representation, which is obtained via the Jordan-Wigner (JW) transformation, i.e., $\hat{c}_j^\dagger = \hat{\sigma}_j^+ (\prod_{m=1}^{j-1} \hat{\sigma}_m^z)$, where $\hat{\sigma}_j^\pm \equiv (\hat{\sigma}_j^x \pm i\hat{\sigma}_j^y)/2$. The couplings $J_{i,j,k,l}$ are zero-mean Gaussian-distributed complex random variables with a variance $\langle\langle J_{i,j,k,l}^2 \rangle\rangle = J^2/N^3$, where $\langle\langle J_{i,j,k,l}^2 \rangle\rangle$ denotes an average over different disorder realizations. This scaling ensures that the SYK battery model of Rossini *et al.* (2020) has a well-defined thermodynamic limit, precluding any potential collective advantage that might have been present if a different normalization was chosen. Note that Eq. (41) differs from the battery Hamiltonian $H_B^{(0)}$ in Eq. (30) since $H_B^{(1)}$ commutes with the battery Hamiltonian in Eq. (30), which cannot inject energy in the system.

This model displays a superextensive scaling of the optimal charging power $\langle P \rangle_\tau \sim N^{3/2}$. Furthermore, a certification of the quantum origin of the charging advantage of the cSYK model is provided by considering the following bound:

$$\langle P \rangle_\tau \leq \sqrt{\langle \Delta E_B^2 \rangle_\tau \langle \Delta E_1^2 \rangle_\tau}, \quad (43)$$

where $\langle \Delta E_B^2 \rangle_\tau$ ($\langle \Delta E_1^2 \rangle_\tau$) is the time-averaged variance of $H_B^{(0)}$ ($H_B^{(1)}$). Equation (43) is a loose version of the bound on the average power derived by Julià-Farré *et al.* (2020). Furthermore, $\langle \Delta E_1^2 \rangle_\tau$ scales linearly in N , while the power enhancement is linked to a quadratic scaling of $\langle \Delta E_B^2 \rangle_\tau$, which hints at a genuine quantum advantage (see Sec. II.C.4) for the cSYK model.

Rossini *et al.* (2020) examined a bosonic version of the SYK battery and a parallel charging scheme, showing that neither model holds a quantum advantage. The poor performance of the bosonic SYK battery compared to the cSYK battery suggests that nonlocal JW strings for fermions are crucial for maximizing entanglement production during time evolution, and therefore correlations between the battery units. This result is in accordance with the bound $P(t) \leq \gamma k N$ derived by Gyhm, Šafránek, and Rosa (2022) that was discussed in Sec. II.C.3, with k the interaction order and γ a constant. When the Hamiltonian in Eq. (42) is represented in the spin basis via the JW transformation a Jordan string $\prod_{m=i}^{i+k} \hat{\sigma}_m^z$ emerges in the Hamiltonian with an interaction order of $k \sim N$. Conversely, when one considers the bosonic SYK model Jordan strings are absent, resulting in an interaction order of $k = 4$.

Rossini *et al.* (2020) provided a quantum many-body battery model where fast charging occurs due to the maximally entangling underlying quantum dynamics envisioned by Binder *et al.* (2015b) and Campaioli *et al.* (2017). Still, the nonlocal interactions peculiar to the SYK model may be extremely challenging to realize in practice, and the feasibility of such a many-body battery remains under dispute; see, however, the discussion in Sec. VI.

D. Work extraction

Most of the previous discussion focused on the scaling of the charging dynamics with the number N of battery units. However, the performance of a battery cannot be captured by a single figure of merit such as the charging power $\langle P \rangle_\tau$. For example, a “good” battery should not only be charged in a small amount of time but also have the capability of fully delivering such energy in a useful way, i.e., to perform work. This ability is measured by the ergotropy \mathcal{E} , which was introduced in Sec. II.A.1. In the context of a many-body battery, the presence of correlations and entanglement between different constituents may induce limitations on the task of energy extraction (Oppenheim *et al.*, 2002). Andolina, Keck, Mari, Campisi *et al.* (2019) studied the maximum work $\mathcal{E}(\tilde{\tau})$ that can be extracted from N TLSs in a Dicke battery, where $\tilde{\tau}$ is the optimal charging time (i.e., the time that maximizes the charging power). It was observed that, for finite-size batteries, the extractable energy $\mathcal{E}(\tilde{\tau})$ constitutes a small fraction of the total energy $E(\tilde{\tau})$ stored in the battery. This reduction is due to the presence of correlations (entanglement) between the charger and the battery, proving that quantum effects can be detrimental for work extraction. However, this issue can be mitigated in the limit of a large

number of battery units since the fraction of energy locked by correlations becomes negligible, i.e., $\lim_{N \rightarrow \infty} \mathcal{E}(\tilde{\tau})/E(\tilde{\tau}) = 1$, regardless of the initial state of the charger.

As further demonstrated by [Rossini, Andolina, and Polini \(2019\)](#), this is a general property of quantum charging processes of closed Hamiltonian systems, which is ultimately linked to the integrability of the dynamics and does not depend on the details of the underlying microscopic model. [Rossini, Andolina, and Polini \(2019\)](#) considered a disordered quantum Ising chain Hamiltonian charged via a direct charging protocol. The quantum Ising Hamiltonian that was studied has a rich equilibrium phase diagram presenting many-body localized (MBL), Anderson localized (AL), and ergodic phases. Here the ergotropy of a subsystem of $M \leq N$ battery units $\mathcal{E}_M(\tilde{\tau})$ properly normalized by the energy of the same subsystem $E_M(\tilde{\tau})$ can be used to discriminate different thermodynamic properties of the eigenstates of the system, as shown in [Fig. 6\(b\)](#). Indeed, considering half of the chain ($M = N/2$), the ratio $\mathcal{E}_{N/2}(\tilde{\tau})/E_{N/2}(\tilde{\tau})$ saturates to a finite constant when the thermodynamic $N \rightarrow \infty$ limit is taken if the ergodic phase is considered. In contrast, in the MBL and AL phases the energetic cost of creating correlations becomes negligible in the thermodynamic limit, i.e., $\mathcal{E}_{N/2}(\tilde{\tau})/E_{N/2}(\tilde{\tau}) \rightarrow 1$. This stems from the fact that in these phases the dynamics is restricted to a subportion of the Hilbert space. The findings of this study demonstrate that ergotropy can effectively distinguish among different thermodynamic phases of a quantum system and reveal insight into its underlying dynamics. The issue of energy extraction was also investigated in waveguide quantum electrodynamics setups ([Monsel *et al.*, 2020](#); [Maffei, Camati, and Auffèves, 2021](#)), in random quantum systems ([Caravelli *et al.*, 2021](#)), and by means of auxiliary subsystems ([Chaki *et al.*, 2023](#)).

IV. CHARGING PRECISION

While powerful energy transfer always seems to be desirable, speed can come at the expense of precision. We now look at some results on the precision of unitary charging and work extraction ([Friis and Huber, 2018](#); [Rosa *et al.*, 2020](#); [Santos *et al.*, 2019](#); [Crescente *et al.*, 2020b](#); [Santos, Saguia, and Sarandy, 2020](#); [Delmonte *et al.*, 2021](#); [Moraes *et al.*, 2021](#); [Abah *et al.*, 2022](#); [Dou, Wang, and Sun, 2022a](#); [Dou *et al.*, 2022](#); [Hu *et al.*, 2022](#); [Imai, Gühne, and Nimmrichter, 2023](#); [Bakhshinezhad *et al.*, 2024](#)), which aim to mitigate work fluctuations.

A. Bosonic batteries and Gaussian unitaries

[Friis and Huber \(2018\)](#) proposed focusing on charging precision and studying a bosonic quantum battery given by an ensemble of harmonic oscillators, i.e., $H_0 = \sum_j \omega_j \hat{a}_j^\dagger \hat{a}_j$, with no charger involved. [Friis and Huber \(2018\)](#) considered a quantum battery in an initial, completely passive state $\rho_0 = G_\beta[H_0] = \otimes_j G_\beta[H_{0,j}]$, where $H_{0,j} = \omega_j \hat{a}_j^\dagger \hat{a}_j$ is the Hamiltonian of the j th mode and

$$G_\beta[H_{0,j}] = (1 - e^{-\beta\omega_j}) \sum_n e^{-n\beta\omega_j} |n_j\rangle\langle n_j|. \quad (44)$$

In [Eq. \(44\)](#) $|n_j\rangle$ is the Fock state with n particles in the j th mode. The system is charged by some unitary U to a final state $\rho = U\rho_0U^\dagger$ such that $W = \text{Tr}[H_0\rho] - \text{Tr}[H_0\rho_0]$ is the energy deposited by U . To quantify the *charging precision*, [Friis and Huber \(2018\)](#) considered two quantities. First, they studied fluctuations in the final energy of the battery using the variance of the internal Hamiltonian with respect to the final state,

$$\Delta E^2(\rho) = \text{Tr}[H_0^2\rho] - \text{Tr}[H_0\rho]^2. \quad (45)$$

Second, they evaluated energy fluctuations ΔW during the charging process using

$$\Delta W^2 = \sum_{m,n} p_{m \rightarrow n} (W_{m \rightarrow n} - W)^2, \quad (46)$$

where $W_{m \rightarrow n} = \text{Tr}[H_0|n\rangle\langle n|] - \text{Tr}[H_0|m\rangle\langle m|]$ is the energy difference between two energy levels m and n and $p_{m \rightarrow n} = p_m |\langle n|U|m\rangle|^2$ is the transition probability from an initial state $|n\rangle$ with population $p_n = \text{Tr}[\rho_0|n\rangle\langle n|]$ to a final state $|m\rangle$ with population p_m .

[Friis and Huber \(2018\)](#) focused on the special class of Gaussian unitaries ([Gardiner and Zoller, 2000](#)) generated by Hamiltonians that are at most quadratic in a_j^\dagger, a_j due to the feasibility of their practical implementation. They showed that neither ΔE nor ΔW is bounded from above or increases with W for infinite-dimensional systems. They then provided lower bounds on ΔE and ΔW for single-mode and multimode systems, presenting the optimal protocols for maximizing charging precision as a function of W and temperature T , respectively. The best Gaussian operations produce energy fluctuations that vanish asymptotically when compared to W for large energy supplies.

Such a clear-cut interpretation is more difficult to obtain in the case of multimode batteries ([Konar, Patra *et al.*, 2022](#)), for which more investigations are needed to clarify the role of coherences and correlations. Further work in this direction could focus on the role of higher-order interactions [i.e., interactions mediated by \hat{a}^n and $(\hat{a}^\dagger)^n$ with $n \geq 1$] in the performance of bosonic batteries ([Delmonte *et al.*, 2021](#)). The charging of bosonic quantum batteries via squeezing is also worth considering, as recently shown by [Centrone, Mancino, and Paternostro \(2023\)](#).

B. Adiabatic quantum charging

[Santos *et al.* \(2019\)](#) proposed an approach to mitigate work fluctuations based on the use of stimulated Raman adiabatic passage (STIRAP) ([Gaubatz *et al.*, 1990](#); [Vitanov *et al.*, 2017](#)), which is akin to transitionless quantum driving ([Berry, 2009](#)). The protocol is based on the idea of slowly varying the interaction Hamiltonian to prevent any undesired transition between its eigenstates. To achieve adiabatic driving, [Santos *et al.* \(2019\)](#) considered a time-dependent interaction Hamiltonian $H_1(t)$ such that $[H_1(0), \tilde{\rho}_0] = 0$, where $\tilde{\rho}_0 = e^{iH_0 t} \rho_0 e^{-iH_0 t}$ is the initial state of the battery in the interaction picture. The interaction Hamiltonian is then slowly changed until some target state $\rho^* = \rho(\tau)$ is reached at a time τ .

Santos *et al.* (2019) studied adiabatic charging for the case of a three-level system, which is well known in the field of STIRAP (Vitanov *et al.*, 2017), using the interaction Hamiltonian $H_1(t) = \Omega_{12}(t)|1\rangle\langle 2| + \Omega_{23}(t)|2\rangle\langle 3| + \text{H.c.}$, where the time-dependent transition frequencies $\Omega_{12}(t) = \Omega_0 f(t)$ and $\Omega_{23}(t) = \Omega_0[1 - f(t)]$ are chosen such that $f(0) = 0$ and $f(\tau) = 1$, with Ω_0 the maximal frequency of the interaction.

Santos *et al.* (2019) compared the energy deposited onto the battery $W(\tau)$ with the bandwidth of the Hamiltonian $W_{\max} := w[H_0] = \epsilon_3 - \epsilon_1$, i.e., the maximal amount of energy that can be deposited onto the battery. They also compared the average charging power $\langle P \rangle = W(\tau)/\tau$ with the maximal achievable power $\langle P \rangle_{\max} := W(\tau)/\tau_{\text{QSL}}$, which they calculated using a Margolus-Levitin form of the QSL in Eq. (12), i.e., $\tau_{\text{QSL}} = \pi/2W_{\max}$. These quantities were studied as a function of the dimensionless parameter $\Omega_0\tau$. As expected, far from adiabaticity, i.e., for $\Omega_0\tau \ll 1$, the battery performs poorly and W/\mathcal{E} , $\langle P \rangle/\langle P \rangle_{\max} \approx 0$. As $\Omega_0\tau$ grows, the energy deposited grows until the battery can be fully charged ($W/\mathcal{E} = 1$). However, the charging power grows until it reaches a maximum value at $\Omega_0\tau \sim 1$ and then decreases for larger values of $\Omega_0\tau$. This result shows a trade-off relation between charging power and precision that is dictated by the competition between adiabaticity and the saturation of the QSLs.

Note that maximal power $\langle P \rangle/\langle P \rangle_{\max} \approx 1$ may be achieved via *shortcuts to adiabaticity* (STAs) (Santos *et al.*, 2019), i.e., by engineering a fast process that leads to the same final state and work fluctuations as in adiabatic processes. However, STAs require more energy due to control interactions Campbell and Deffner (2017), thus affecting the efficiency of the protocol (Uzdin *et al.*, 2012; Campaioli *et al.*, 2019).

The promising role of adiabatic driving in quantum batteries was demonstrated in an experiment by Hu *et al.* (2022) (see Sec. VI) and the protocols proposed by Dou, Wang, and Sun (2020), Santos, Saguia, and Sarandy (2020), Moraes *et al.* (2021), and Dou, Wang, and Sun (2022a, 2022b). Outlooks should focus on the trade-off among the charging power, precision, and energetic cost of the charging protocol. The relation between the speed of evolution and the cost of STAs was studied by Santos and Sarandy (2015) and Campbell and Deffner (2017). Extending these works by explicitly accounting for finite deviations from adiabaticity could clarify the feasibility of powerful and precise charging. Another interesting direction could be to jointly optimize charging power and precision by choosing a suitable target function $\mathcal{F}(\langle P \rangle, W, \delta W)$ (Binder *et al.*, 2015b).

C. Entanglement and work fluctuations

Fabrication defects and other sources of noise introduce disorder in the energies of each subsystem and in the couplings between them. In the presence of disorder, unitary dynamics is characterized by temporal fluctuations that manifest at different timescales. These fluctuations affect $W(t)$ and need to be mitigated to improve charging precision. Rosa *et al.* (2020) focused on these fluctuations and showed that they can be suppressed by preparing many-body quantum batteries in highly entangled states. Note that in practice entanglement in many-body systems is usually fragile due to an exponentially fast suppression of correlations as an effect

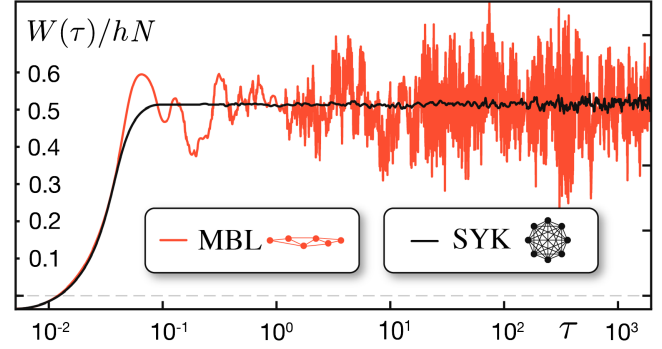


FIG. 7. Temporal fluctuations affecting the charging precision can be suppressed in many-body quantum batteries by promoting the formation of volume-law entanglement. Work fluctuations in SYK batteries (black line) are exponentially suppressed over all timescales as localized states transition to highly entangled states. Instead, MBL quantum batteries are characterized by localized states and exhibit large work fluctuations at all timescales. Adapted from Rosa *et al.*, 2020.

of decoherence. Therefore, the feasibility of the protocol introduced by Rosa *et al.* (2020) depends on the ability to sustain highly entangled states.

Rosa *et al.* (2020) considered the local N -spin battery model in Eq. (8) with $H_j = h\hat{\sigma}_j^z$, where h represents the energy scale of each subsystem. The battery is charged via the direct charging protocol in Eq. (25). They considered two different models for the interaction $H_1^{(N)}$,

$$H_{\text{MBL}}^{(N)} = \sum_{j=1}^N (J_j \hat{\sigma}_j^x \hat{\sigma}_{j+1}^x + J_2 \hat{\sigma}_j^x \hat{\sigma}_{j+2}^x), \quad (47)$$

$$H_{\text{SYK}}^{(N)} = \sum_{i < j < k < l} J_{i,j,k,l} \hat{\gamma}_i \hat{\gamma}_j \hat{\gamma}_k \hat{\gamma}_l, \quad (48)$$

where J_j and J_2 are the nearest-neighbor and next-to-nearest-neighbor Ising couplings and $\hat{\gamma}_i$ is the Majorana fermion operator.¹¹ Together with the internal Hamiltonian $H_0^{(N)}$ the many-body localized Hamiltonian $H_{\text{MBL}}^{(N)}$ is a model for many-body quantum systems that exhibits different quantum phases (eigenstate thermalization hypothesis, Anderson localized, many-body localized, and spin-glass phases) depending on the value of its parameters (Kjäll, Bardarson, and Pollmann, 2014; Nandkishore and Huse, 2015). The SYK Hamiltonian $H_{\text{SYK}}^{(N)}$, which was discussed in Sec. III.C.2, is characterized by nonlocal interactions that promote the formation of highly entangled states (Rosa *et al.*, 2020).

Rosa *et al.* (2020) studied fluctuations in $W(\tau)$ relative to the Hamiltonian bandwidth Nh using the parameter $R(\tau) = W(\tau)/Nh$. They showed that fluctuations of $R(\tau)$ were suppressed in the presence of nonlocal correlations (see Fig. 7), with an amplitude that decreases with the number of subsystems N involved. Rosa *et al.* (2020) provided extensive mathematical evidence to support the thesis that energy

¹¹It holds that $\hat{\gamma}_i = \hat{\gamma}_i^\dagger$ and $\{\hat{\gamma}_i, \hat{\gamma}_j\} = \delta_{ij}$.

fluctuations in $W(\tau)$ are mitigated by the rapid and homogeneous formation of highly entangled states over many energy levels (volume-law entanglement), which is typical of the SYK Hamiltonian and other models for quantum chaos (Bianchi *et al.*, 2022).

Rosa *et al.* (2020) linked the exponential suppression of stored-energy fluctuations at all timescales to the collective nonlocal thermalization of chaotic systems. An interesting outlook is to test their conjecture that the SYK model sets an upper bound on the precision of quantum batteries. Since SYK models can provide both powerful and precise charging (Rosa *et al.*, 2020; Rossini *et al.*, 2020), further work in this direction should focus on experimentally viable SYK charging architectures; see Sec. VI. The relation between entanglement and work fluctuations was also considered by Caravelli *et al.* (2021) and Imai, Gühne, and Nimmrichter (2023). Furthermore, quantum control (Mazzoncini *et al.*, 2023; Rodríguez *et al.*, 2024) could be used to generate fluctuation-free active states in many-body systems based on more experimentally feasible models, as done for *entanglement storage* by Caneva, Calarco, and Montangero (2012).

V. OPEN QUANTUM BATTERIES

An *open quantum battery* (OQB) is an open quantum system that may be charged by an auxiliary system, i.e., the charger, denoted by \mathbf{C} and/or may interact with the external environment, denoted by \mathbf{E} . If the battery system is isolated, closed, or perfectly protected from the outside, then it will evolve unitarily as in Eq. (2). Conversely, the dynamics of an OQB is generated by the Hamiltonian of the universe H , whose microscopic details may not be fully accessible,

$$H = H_{\mathbf{B}} + H_{\mathbf{C}} + H_{\mathbf{E}} + H_{\text{int}}, \quad (49)$$

where the interaction terms H_{int} may couple the battery, charger, and environment to each other. In this regard, we are going to propose the wording *dissipative quantum battery* (DQB) to denote more specifically an OQB subject to an external environment \mathbf{E} that is usually unknown, uncontrollable, and whose degrees of freedom far outnumber those of the battery and charger subsystem (Carrega *et al.*, 2020; Carrasco *et al.*, 2022).

The dynamics of an open battery can be described using density operator master equations (Breuer and Petruccione, 2002) such as the general Liouville–von Neumann equation $\dot{\rho}_{\mathbf{B}}(t) = \mathcal{L}_t[\rho_{\mathbf{B}}(t)]$, where \mathcal{L}_t is a time-dependent superoperator. The latter prescribes the dynamics of the battery’s density operator $\rho_{\mathbf{B}}(t) = \Lambda_{t,0}[\rho_{\mathbf{B}}(0)]$, which approximates the underlying process

$$\rho_{\mathbf{B}}(t) = \text{Tr}_{\mathbf{CE}}[\rho(t)] = \text{Tr}_{\mathbf{CE}}[U(t;0)[\rho_0]], \quad (50)$$

where $\rho(t)$ is the state of the universe at time t starting from an initial state ρ_0 . The unitary map $\mathcal{U}_{t,0}[\cdot] = U(t;0) \cdot U(t;0)^\dagger$ is generated by the total Hamiltonian H such that $U(t;0) = \mathcal{T}\{\exp[-i\int_0^t ds H(s)]\}$. The dynamics of OQBs have been studied extensively in the Markovian regime (Farina *et al.*, 2019; Gherardini *et al.*, 2020; Quach and Munro, 2020) using

the Gorini-Kossakowski-Sudarshan-Lindblad (GKSL) quantum master equation (Chruściński and Pascazio, 2017),

$$\dot{\rho}_{\mathbf{B}}(t) = -i[H_{\mathbf{B}}, \rho_{\mathbf{B}}(t)] + \mathcal{D}[\rho_{\mathbf{B}}(t)], \quad (51)$$

where $\mathcal{D}[\rho] = \sum_k \gamma_k (\hat{L}_k \rho \hat{L}_k^\dagger - \{\hat{L}_k^\dagger \hat{L}_k, \rho\}/2)$ is a superoperator modeling the interaction between the battery and the rest of the universe, via a set of operators \hat{L}_k generating incoherent transitions at rates γ_k (Breuer and Petruccione, 2002). Some have also considered OQBs beyond the Markovian approximation (Kamin, Tabesh, Salimi, Kheirandish, and Santos, 2020; Ghosh *et al.*, 2021; Morrone *et al.*, 2023), where memory effects become important for a complete description of the dynamics.

DQBs are subject to decoherence and energetic relaxation, which tend to deteriorate resourceful active states, leading them toward passive (via dephasing or depolarization) or even completely passive states (via thermalization). If these processes are not properly prevented, their timescale puts a limit on the lifetime of the active states and thus on how long the DQB can keep its charge. Furthermore, the performance of some DQB models can decrease over time when many charging-discharging cycles are performed in an aging process analog to that of electrochemical batteries (Pirmoradian and Mølmer, 2019).

For these reasons, protection mechanisms from relaxation are essential for device implementation (Bai and An, 2020; Xu *et al.*, 2022); they are reviewed in Secs. V.B and V.C. This issue was addressed originally by Liu, Segal, and Hanna (2019), Gherardini *et al.* (2020), and Quach and Munro (2020) and later by Mitchison, Goold, and Prior (2021), Yao and Shao (2021), and Yao and Shao (2022), while Camati *et al.* (2016), Batalhão *et al.* (2019), and Landi and Paternostro (2021) focused on the thermodynamics of DQB stabilization.

A. Charging a dissipative quantum battery

1. Dissipative charging

A dissipative charging scheme was proposed by Barra (2019) and extended by Hovhannisyanyan, Barra, and Imperato (2020) and Chang *et al.* (2021). Barra (2019) proposed engineering a dissipative process that involves an ensemble of auxiliary quantum systems A , all initialized in a thermal Gibbs state $G_\beta[H_A]$ at some temperature $(k_B\beta)^{-1}$. A sequence of interactions between the battery and individual elements of this ensemble is then used to drive the battery’s state to an active equilibrium π (Kamin *et al.*, 2023), i.e., an equilibrium state with positive ergotropy ($\mathcal{E}[\pi] > 0$). This is akin to collisional models, which were applied to DQBs by Guarnieri *et al.* (2020), Landi (2021), Seah *et al.* (2021), Barra (2022), Chen *et al.* (2022), Ciccarello *et al.* (2022), Shaghaghi *et al.* (2022, 2023), and Salvia *et al.* (2023).

Barra (2019) coupled the battery with an auxiliary subsystem A via a time-independent interaction V for a time interval τ during which the battery’s state evolves as $\rho \rightarrow \rho' = \text{Tr}_A[U\rho \otimes G_\beta[H_A]U^\dagger] =: \Phi[\rho]$, with $U = \exp[-i(H_{\mathbf{B}} + H_A + V)]$. This implicitly defines a dissipative dynamical map Φ on the battery, which is assumed to have a unique fixed point π such

that $\Phi[\pi] = \pi$ and $\lim_{n \rightarrow \infty} \Phi^n[\rho_0] = \pi$ for any initial state of the battery ρ_0 .

Any unitary operator U associated with a map with equilibrium satisfies $[U, H'_B + H_A] = 0$ for some Hamiltonian H'_B on the battery's space such that $\pi = G_\beta[H'_B]$ (Barra and Lledó, 2017). Now, if $H'_B = H_B$, then π is a completely passive state and $\mathcal{E}[\pi] = 0$. Instead, if $H'_B \neq H_B$, the equilibrium π may be active with respect to the bare Hamiltonian of the battery H_B , leading to $\mathcal{E}[\pi] > 0$. Barra (2019) obtained a general condition for reaching an active equilibrium, which stems from the fact that $[U, H'_B + H_A] = 0$ if $[H_B, H'_B] = 0$ and $[H'_B + H_A, V] = 0$. They concluded that π is an active equilibrium if there is a pair (i, j) such that $(\epsilon_i - \epsilon_j)(\epsilon'_i - \epsilon'_j) \leq 0$, with ϵ_i and ϵ'_i the eigenenergies of H_B and H'_B , respectively.

While it is clear what H'_B should be used for π to be active in H_B , such as $H'_B = -H_B$, the power of the result by Barra (2019) is that it provides a prescription for the interaction V to obtain an effective Hamiltonian H'_B with an associated active equilibrium π . They showed that a generic interaction $V = \sum_\alpha \hat{B}_\alpha \otimes \hat{A}_\alpha$ leads to an active state if the battery (auxiliary) interaction operators \hat{B}_α (\hat{A}_α) satisfy $[H_B, \hat{B}_\alpha] = \lambda_\alpha \hat{B}_\alpha$ ($[H_A, \hat{A}_\alpha] = \lambda_\alpha \hat{A}_\alpha$) for some $\{\lambda_\alpha\}$, leading to $H'_B = -H_B$.

Barra (2019) also examined the energetic cost of charging W_{ch} associated with performing such repeated interactions V leading to π . They obtained $W_{\text{ch}} = \text{Tr}[(H_B - H'_B)(\pi - \rho_0)]$, which vanishes if π is a thermal equilibrium state of H_B . They were then able to quantify the efficiency η of the associated charging process, which was given as the ratio between the ergotropy of π and the cost of the charging process,

$$\eta := \frac{\mathcal{E}[\pi]}{W_{\text{ch}}} = 1 - \frac{|Q_{\text{ch}}|}{W_{\text{ch}}}, \quad (52)$$

in agreement with the second law of thermodynamics and in analogy with the Carnot limit, where $Q_{\text{ch}} = \text{Tr}[H'_B(\pi - \sigma_\pi)]$ is the total heat exchanged, with σ_π the passive state of π .

These results outline a trade-off between the charging efficiency η and the ergotropy \mathcal{E} . Hence, one cannot maximize both at the same time, and this is a general property of thermalization-assisted charging (Barra, 2019; Hovhannisyan, Barra, and Imperato, 2020).

2. Environment-assisted charging

The charging mechanism described in Sec. V.A.1 can be generalized by relaxing the condition on π to be thermal, which may be attained for a more structured environment, where a charger can also be included. The proposed approaches can be classified as follows: first, the case of charging assisted by non-Markovian effects (Kamin, Tabesh, Salimi, Kheirandish, and Santos, 2020; Ghosh *et al.*, 2021) and, second, the benefits of engineering the interactions between the battery and the external environment (Tabesh, Kamin, and Salimi, 2020; Xu *et al.*, 2021; Xu *et al.*, 2023). In both cases the environment is at least partly known, so some modeling of the experimental data can be built.

We begin with charging assisted by non-Markovian effects. Kamin, Tabesh, Salimi, Kheirandish, and Santos (2020) showed that both the battery and the charger are given by

TLSs resonantly coupled and interacting with an independent environment. The latter is given by an amplitude damping reservoir, modeled as an ensemble of quantum harmonic oscillators. Kamin, Tabesh, Salimi, Kheirandish, and Santos (2020) determined that in the underdamped regime¹² the presence of the environment leading to non-Markovian effects allows for the optimal energy transfer from the charger to the battery. Thus, albeit the environment \mathbf{E} generally degrades the charging of the battery, there are parameter regimes where the charging performance is close to ideal.

Ghosh *et al.* (2021) considered a case study where the presence of an external noise source leading to non-Markovian effects effectively improves the performance of the charging process with respect to the noiseless case. The key difference found by Kamin, Tabesh, Salimi, Kheirandish, and Santos (2020) was that both the battery and the charger are quantum many-body systems. Specifically, Ghosh *et al.* (2021) initially prepared the battery as the ground state of a one-dimensional XY model with a transverse magnetic field in open boundary conditions, and the battery was charged and discharged via interactions with local bosonic reservoirs. In the transient regime, the DQB can store energy faster and return a higher ergotropy if it is affected by non-Markovian dephasing noise.

A complementary scenario is that of engineered battery-environment interactions. Xu *et al.* (2021) also considered a battery and the charger given by the TLS and showed that, by tuning the spectral density function (SDF) of the environment, the performance of the charging process increases when a stronger coupling strength with the environment is enabled in the so-called band-gap configuration. In other words, the SDF consists of positive- and negative-weighted Lorentzian spectra centered around the same frequency. In this condition, one can fully charge the DQB and extract the total stored energy as useful work. Another approach, proposed by Tabesh, Kamin, and Salimi (2020), consisted of a battery and a charger that were not directly coupled but were allowed to interact through a common environment. Quach and Munro (2020) took a similar approach in which the battery was charged more efficiently with a strong battery-environment interaction.

B. Active charging and stabilization methods

1. Controllability of closed and open quantum batteries

The charging and stabilization of QOBs can be framed as *control tasks*, whereby some control operations are used to increase the energy of the battery with respect to its internal Hamiltonian H_B and then protect it from leaking back into the environment. For isolated and closed quantum batteries, we are asking for the existence of a unitary operator $U(\tau; 0)$ so that $\rho(\tau) = \mathcal{U}(\tau; 0)[\rho_0] = |e\rangle\langle e|$. If such a unitary operator $U(\tau; 0)$ does not exist, one can relax the control requirements of the charging process. For example, one could vary the target time τ or choose a different target state ρ^* from the maximally charged state associated with H_B . Alternatively, we

¹²The interaction between the battery and the charger is stronger than the coupling among such single quantum systems and the common environment.

can still seek full charging $|e\rangle \rightarrow |g\rangle$ by opening the quantum battery to external resources. This can be achieved via the charger (Ferraro *et al.*, 2018; Farina *et al.*, 2019), as seen in Sec. III.B for the case of the Dicke quantum battery. A charger can be employed regardless of whether the battery is interacting with the external environment. However, in the presence of a dissipative environment (Carrega *et al.*, 2020; Carrasco *et al.*, 2022) one would seek conditions to guarantee that the charging process is energetically efficient, despite the effect of dissipation.

In the current literature, several solutions have been proposed to realize a charger. Among the most meaningful have involved a thermal heat engine (Levy, Diósi, and Kosloff, 2016; Son, Talkner, and Thingna, 2022), an external quantized light field (Ferraro *et al.*, 2018; Andolina, Keck, Mari, Campisi *et al.*, 2019; Monsel *et al.*, 2020), an ancilla system acting as a controllable switch (Farina *et al.*, 2019), and a stream of coherently prepared quantum units (Landi, 2021; Seah *et al.*, 2021; Salvia *et al.*, 2023).

2. Stabilization power and its energy cost

We now consider a scenario where we charge a DQB onto the maximally charged state $\rho^* = |e\rangle\langle e|$ from an arbitrary initial quantum state at the desired time τ and stabilize ρ^* for an arbitrarily long time until the external user requests the stored energy. For such a purpose, unitary operations are no longer sufficient since they are *isentropic* (and thus adiabatic and reversible) processes and cannot decrease the entropy changes induced by E . Hence, a nonunitary operation is needed, requiring an extra energy cost, named the stabilization cost, due to the use of auxiliary systems.

For these strategies to be energetically favorable, the stabilization cost W_{stab} must be smaller than the energy storage capacity $E_{\text{max}} = \text{Tr}[H_B(\rho^* - |g\rangle\langle g|)]$. To this end, Gherardini *et al.* (2020) introduced two figures of merit: the instantaneous *relative stabilization cost*

$$\eta_{\text{stab}}(t) := \frac{W_{\text{stab}}(t)}{E_{\text{max}}} \quad (53)$$

and the instantaneous *relative excess stabilization cost*

$$\zeta_{\text{stab}}(t) := \frac{W_{\text{stab}}(t) - \mathfrak{L}(t)}{E_{\text{max}}} \quad (54)$$

that identifies the excess cost besides the total amount of energy spent to compensate the energy leakage $\mathfrak{L}(t)$ due to decoherence and thermalization. For open dynamics described by the GKSL equation (51), $\mathfrak{L}(t) := \text{Tr}[H_B \mathcal{D}[\rho_B(t)]]$. Ideally one should allow for $W_{\text{stab}}(t) = \mathfrak{L}(t)$ such that $\eta_{\text{stab}}(t) = \mathfrak{L}(t)/E_{\text{max}}$ and $\zeta_{\text{stab}}(t) = 0$ for any time t , so the energy needed to stabilize the DQB is minimized. This intuitive result can be analytically demonstrated with thermodynamics arguments (Gherardini *et al.*, 2020).

The power $P_{\text{stab}}(t) := \dot{W}_{\text{stab}}(t)$ in stabilizing a DQB has a lower bound (Gherardini *et al.*, 2020) that determines the minimum amount of energy that has to be supplied from the outside. The lower bound derives from the first law of thermodynamics (Horowitz and Jacobs, 2015),

$$\dot{E}(t) = \dot{W}_{\text{stab}}(t) + \mathcal{J}_{E \rightarrow B}(t), \quad (55)$$

where $E(t) = \text{Tr}[H_B(t)\rho_B(t)]$ is the instantaneous total battery energy,¹³ while $\mathcal{J}_{E \rightarrow B}(t) := \dot{E}_{\text{EB}}(t)$ denotes the instantaneous energy current driven into the battery by the external environment. It can thus be shown (Gherardini *et al.*, 2020) that the stabilization power $P_{\text{stab}}(t)$ follows the inequality

$$P_{\text{stab}}(t) \geq \dot{E}(t) - T_\pi \dot{S}[\rho_B(t)], \quad (56)$$

where T_π is an effective temperature able to parametrize π , the invariant state of the DQB under the influence of the environment.¹⁴ In case the open dynamics of the battery is governed by Eq. (51), then $\dot{S}[\rho_B(t)] = -\text{Tr}[\mathcal{D}[\rho_B(t)] \log \rho_B(t)]$.

The lower bound of Eq. (56) also entails an inequality on the time derivative of the nonequilibrium free energy $F(t) := E_{\text{EB}}(t) - T_\pi S[\rho_B(t)]$ for the battery without the charger and the controller. This inequality reads $\dot{F}(t) \leq 0$, where the nonequilibrium free energy $F(t)$ reduces over time due to the increase of the battery von Neumann entropy. Hence, the action of the control procedure assisting the charger is to invert this time behavior of $F(t)$. As a consequence, the *minimum stabilization power* is the one allowing for $\dot{F}(t) = 0$ (i.e., constant nonequilibrium free energy), such that the entropy due to the environment is perfectly compensated by the control. Therefore, Eq. (56) implicitly indicates that the *minimum energy cost* to stabilize a DQB is proportional to $E(t) - T_\pi S[\rho_B(t)]$.

3. Charging and stabilization via sequential measurements

Gherardini *et al.* (2020) introduced a control strategy for the stabilization of a DQB given by a nonunitary open-loop control that requires a sequence of projective energy measurements to be performed at discrete consecutive times (Gherardini, 2019; Gherardini *et al.*, 2021). The energy measurements have to be close enough in time that the dynamics of the DQB is frozen in the corresponding energy basis, which is in agreement with the *quantum Zeno regime* (Smerzi, 2012; Müller *et al.*, 2016). In this way the energy basis becomes a decoherence-free subspace, and the DQB is stabilized in the maximally charged state¹⁵ $\rho_e := |e\rangle\langle e|$. Albeit maintaining the quantum Zeno regime imposes stringent constraints (Smerzi, 2012; Gherardini *et al.*, 2016; Müller *et al.*, 2016), the time intervals among projective measurements can be optimized to minimize the stabilization power P_{stab} .

As shown in Fig. 8, the protocol of Gherardini *et al.* (2020) consists of three steps.

¹³Assuming that the ground state has zero energy.

¹⁴If the battery is a TLS or the invariant state π is thermal, then the parametrization is exact. Otherwise, the value of T_π can be determined by setting further constraints on the energy or the entropy associated with π (Salvia and Giovannetti, 2020). Another possibility to set the value of T_π is to invoke the concept of *virtual temperatures* (Brunner *et al.*, 2012).

¹⁵The DQB is repeatedly brought back to $|e\rangle\langle e|$ with a much greater probability, as $\rho_B(t)$ and $|e\rangle\langle e|$ are statistically indistinguishable; i.e., their difference is detectable by no measurement devices (Wootters, 1981).

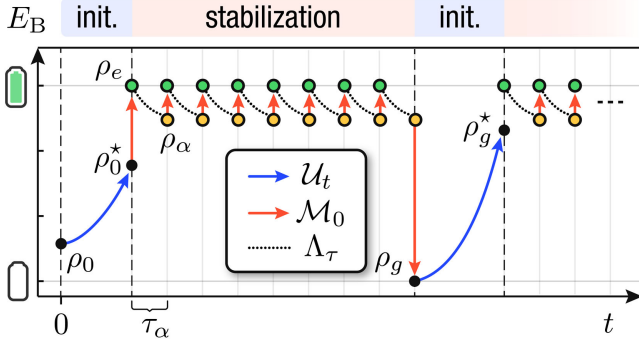


FIG. 8. Single-run pictorial representation of a sequential measurement protocol for a TLS battery. After the initialization step from the initial state ρ_0 , the stabilization protocol consists of intermittent free evolutions, fast unitary controlled dynamics \mathcal{U}_t (solid blue lines), and projective measurements \mathcal{M}_0 (solid red lines) in time intervals of a duration τ . The green dots denote the maximally charged state ρ_e , while the yellow dots represent the battery state ρ_α into which the DQB decays as an effect of the environmental action Λ_τ , here exaggerated for illustrative purposes. Finally, ρ_0^* and ρ_g^* are the nearest states to ρ_e on the unitary orbit of ρ_0 and $\rho_g = |g\rangle\langle g|$, respectively. Adapted from Gherardini *et al.*, 2020.

(i) *Initialization*. Any initial state of the battery $\rho_0 := \rho_B(0)$ is driven to the unitarily connected state that is closest to ρ_e , here denoted as ρ_0^* . This transformation is allowed by controlling the battery through a time-dependent Hamiltonian as in Eq. (2).

(ii) *Full charging and stabilization via projective energy measurements*. Once the battery is in ρ_0^* , a projective energy measurement (defined in the eigenbasis of H_B) is performed. The battery's state collapses into the maximally charged state $|e\rangle$ with a probability $p_e[\rho_0^*] = \text{Tr}[\rho_0^* \rho_e]$. Subsequently the interaction with the environment leads the battery to the lower-energy state $\rho_\alpha = \Lambda_{\tau_\alpha}[\rho_e]$. A sequence of projective measurements \mathcal{M}_0 on the basis of the battery Hamiltonian H_B repeatedly takes the battery to the state $\rho_\alpha \xrightarrow{\mathcal{M}_0} \rho_e$ at consecutive times with the probability $p_e[\rho_\alpha]$. For the protocol to be successful, the time τ_α between subsequent measurements must be much smaller than the timescale of both the battery free evolution and the decoherence time dictated by E.

(iii) \rightarrow (i) *Reinitialization*. When a projective measurement collapses ρ_α onto the ground state $|g\rangle\langle g|$, a new initialization is performed by applying unitary driving as in step (i).

For an unstable DQB, attaining this quantum Zeno regime allows for full charging and stabilization at the price of extra energetic and entropic costs. On average, no energetic cost is associated with the jumps of the projective energy measurements, independently of which the quantum state is measured. However, there is a cost associated with storing and erasing the information associated with these measurements that is connected to the entropic cost of the protocol. Let $p_k[\sigma]$ be the probability for some d -level battery's state σ to collapse onto one of its energy eigenstates ϵ_k . These probabilities carry the informational content of the outcomes obtained by measuring the state σ . The storing and erasure of each measurement outcome requires an entropy production whose rate of change over time is proportional to the time derivative of the Shannon entropy $S_{\text{Sh}}[\sigma] := -\sum_k p_k[\sigma] \log p_k[\sigma]$.

Hence, implicitly as an effect of *Landauer's principle* (Landauer, 1961; Bérut *et al.*, 2012; Zhen *et al.*, 2021), the irreversible erasure of the measurement information content is responsible for an energetic cost W_{Zeno} . Formally

$$W_{\text{Zeno}} = \bar{m} \beta_{\text{eras}}^{-1} S_{\text{Sh}}[\rho_\alpha], \quad (57)$$

where \bar{m} denotes the average number of projections in the quantum Zeno regime [step (ii)] and β_{eras} is the inverse temperature of the macroscopic system that erases the memory containing the measurement outcomes.

4. Charging and stabilization with feedback control

Another approach to charging and stabilization consists in using *linear feedback*, as proposed by Mitchison, Goold, and Prior (2021). They considered a finite-dimensional battery and showed that feedback (or closed-loop) control can fully charge the battery by monotonically increasing its average total energy. They also showed that this protocol can be used to keep the battery in a charged state $\rho_B(t) = \rho^*$ despite the presence of the environment E. Note that feedback asymptotically makes the target state a nonequilibrium steady state that is robust to small additional (i.e., not explicitly modeled) thermal noise.

The procedure proposed by Mitchison, Goold, and Prior (2021) used homodynelike continuous measurements and linear feedback control (Belavkin, 1987; Wiseman and Milburn, 1993; Wiseman, 1994). A finite-dimensional quantum battery was coupled to a two-level quantum charger that pumped energy into the battery. In the following, σ_C^i , with $i = x, y, z$, denotes the standard Pauli operators acting on the charger. The battery resonantly exchanges energy with the charger via the interaction Hamiltonian $H_1 = g(\hat{s}_B \hat{\sigma}_C^+ + \hat{s}_B^\dagger \hat{\sigma}_C^-)$, where g is the battery-charger coupling strength, $\hat{\sigma}_C^\pm := (\hat{\sigma}_C^x \pm i\hat{\sigma}_C^y)/2$, and $\hat{s}_B := \sum_{k=1}^{d-1} |k-1\rangle\langle k|$ denotes the lowering operator for the battery.

The bare Hamiltonian $H_B + H_C$, with $H_C = \hat{\sigma}_C^z/2$, commutes with H_1 : $[H_B + H_C, H_1] = 0$. Thus, the local energy of both the battery and the charger does not change on average. Instead, $\omega_0 \propto \|H_B + H_C\|_{\text{op}}$ is taken as the largest energy scale of the composite battery-charger system. While the battery is considered a well-isolated system, the charger is coherently driven via the Rabi Hamiltonian $H_{\text{drive}}(t) = \Omega(t)\hat{\sigma}_C^y$, with $\Omega(t) \gg \omega_0 \forall t$, in the interaction picture with respect to $H_B + H_C$ and in the rotating wave approximation. The external environment, which is represented by a multimode field, induces spontaneous emission from the charger. Therefore, in the absence of feedback control, the composite battery-charger system evolves following a driven-dissipative dynamics.

The linear feedback control discussed by Mitchison, Goold, and Prior (2021) consists of measuring the photons that are spontaneously emitted by the charger via homodyne detection. The latter returns the signal

$$r(t)dt = \text{Tr}[\rho_{\text{BC}}(t|r)\hat{\sigma}_C^x]dt + \frac{d\omega(t)}{\sqrt{\epsilon\gamma}}, \quad (58)$$

with γ the spontaneous emission rate, ς the measurement efficiency, and $\rho_{\text{BC}}(t|r)$ the instantaneous state of the battery-charger system conditioned on the measurement outcome r . The Wiener increment $d\omega(t)$ models the noise in the detector output that makes the measurement signal a stochastic process. The feedback loop, therefore, is closed by applying a driving field directly proportionally to the measurement record to the charger: $\Omega(t) = \Omega_0 - fr(t - \tau)$, where $\tau > 0$ is the lag in the feedback loop, f is the feedback strength, and Ω_0 is a constant function.

In the nearly ideal case of negligible feedback lag $\tau \approx 0$, the dynamics of the battery subject to feedback is well described by a Markovian GKSL master equation for the ensemble-averaged density operator $\bar{\rho}_{\text{BC}}(t) := \mathbb{E}_r[\rho_{\text{BC}}(t|r)]$, with $\mathbb{E}_r[\cdot]$ denoting the average over the detector noise. For $\tau > 0$ the Markovian description is no longer valid. Hence, in such a case one needs to solve a stochastic Ito equation and then average over several realizations of the corresponding quantum dynamics (Mitchison, Goold, and Prior, 2021).

In the ideal case of noiseless measurement signals (i.e., the maximum measurement efficiency ς) and instantaneous feedback, a battery can be fully charged. Nevertheless, Mitchison, Goold, and Prior (2021) found that a good performance of the charging process and battery stabilization are observed even under more realistic constraints of inefficient measurements and the time delay τ in the feedback loop. However, for sufficiently large τ the control action stops counteracting both the measurement backaction and the detrimental presence of the environment on the charger. As a result, the feedback loop breaks and behaves as a random sequence of quantum measurements (Gherardini *et al.*, 2021) such that the charger relaxes to the maximally mixed state, which is equivalent to a thermal state at infinite temperature.

Further studies on measurement-based stabilization could focus on the evaluation of its energetic and entropic cost (Mitchison, Goold, and Prior, 2021; Yao and Shao, 2021, 2022; Morrone, Rossi, and Genoni, 2023; Yan and Jing, 2023), precision, work extraction, and autonomy (Mitchison, 2019; Hernández-Gómez *et al.*, 2022).

C. Protection from energy losses

We now discuss some approaches based on the preparation of active states that are protected from the environment (Liu, Segal, and Hanna, 2019; Quach and Munro, 2020; Liu and Segal, 2021). These methods do not require energy expenditure following state preparation, in contrast to the previously discussed active stabilization methods.

1. Protection via decoherence-free subspaces

Liu, Segal, and Hanna (2019) proposed an approach to engineer loss-free open quantum batteries, i.e., OQB that are protected from losing energy to the environment. Their scheme consisted of preparing the battery in some energetically favorable state of a decoherence-free subspace (DFS). The latter is a subset of the states space that is protected from decoherence in which the dynamics is perfectly unitary and unaffected by the environment (Lidar and Birgitta Whaley, 2003). DFSs have been extensively studied in the theory of

open quantum systems and quantum information (Zanardi and Rasetti, 1997) as a promising mean to shield quantum states from noise sources that limit the performance of quantum computing (Lidar, Chuang, and Whaley, 1998; Bacon *et al.*, 2000; Beige *et al.*, 2000) and quantum key distribution (Walton *et al.*, 2003). This strategy can also be used to prevent energy loss by engineering a relaxation-free subspace (de Ponte, Mizrahi, and Moussa, 2007), i.e., a DFS unaffected by thermal relaxation.

The working principle of the loss-free battery of Liu, Segal, and Hanna (2019) is based on the decomposition of the battery's Hilbert space into subspaces that are invariant with respect to the dynamics induced by the total Hamiltonian. Following Liu, Segal, and Hanna (2019), we now consider a system (battery) described by a quantum network Hamiltonian

$$H_{\text{B}} = \sum_j E_j |j\rangle\langle j| + \sum_{(j,k)} (J_{jk} |j\rangle\langle k| + \text{H.c.}), \quad (59)$$

where E_j is the energy of each site in the network and J_{jk} is the coupling between pairs of sites (j, k) . Liu, Segal, and Hanna (2019) considered an environment given by a bath of uncorrelated, harmonic vibrational modes coupled to the system only via a subset \mathcal{S} of site operators $|j\rangle\langle j|$, here associated with surface sites. If there is a unitary symmetry operator $\hat{\Pi}$ such that

$$[\hat{\Pi}, H_{\text{B}}] = 0, \quad [\hat{\Pi}, |j\rangle\langle j|] = 0 \quad \forall |j\rangle\langle j| \in \mathcal{S}, \quad (60)$$

then $\hat{\Pi}$ and H_{B} admit a common eigenbasis $\{|\psi_{\alpha}^{(k)}\rangle\}$, where the index α is associated with eigenvalues λ_{α} whose degeneracy d_{α} is spanned by an index $k = 1, \dots, d_{\alpha}$. Under these conditions one can decompose the system's Hilbert space $\mathcal{H}_{\text{B}} = \bigoplus_{\alpha} \mathcal{H}_{\text{B},(\alpha)}$ such that the dynamics generated by the total system-environment Hamiltonian $H_{\text{B}} + H_{\text{int}} + H_{\text{E}}$ leaves these subspaces $\mathcal{H}_{\text{B},(\alpha)}$ invariant (Lidar and Birgitta Whaley, 2003).

To illustrate this approach, Liu, Segal, and Hanna (2019) considered a network with six sites with ring topology (Trudeau, 1994; Thingna, Manzano, and Cao, 2016); see Fig. 9. This system, which is similar to the tight-binding model of a benzene molecule (Bancewicz, Dierksen, and Karwowski, 1989), can be realized with excitonic (Mikhnenko, Blom, and Nguyen, 2015; Jang and Mennucci, 2018; Alicki, 2019) and superconducting architectures (Blais *et al.*, 2021), as well as on other quantum technology platforms. This system can be engineered to have two dark states¹⁶ $|\psi_{\pm}\rangle$ that are not subject to decoherence or relaxation. Specifically, if the composite system is initialized in a state $\rho_0 = |\psi_{\pm}\rangle\langle\psi_{\pm}| \otimes \rho_{\text{E}}$, then the battery will remain in the state $|\psi_{\pm}\rangle\langle\psi_{\pm}|$ at all times.

We now mention a few considerations. First, the robustness of dark states depends on how well the conditions of Eq. (60) are met. Their lifetime depends on the magnitude of the disorder affecting the energies and couplings, as well as on the temperature and the strength of the coupling with the

¹⁶In analogy with the optically dark states that arise under similar conditions in coupled TLSs interacting with light.

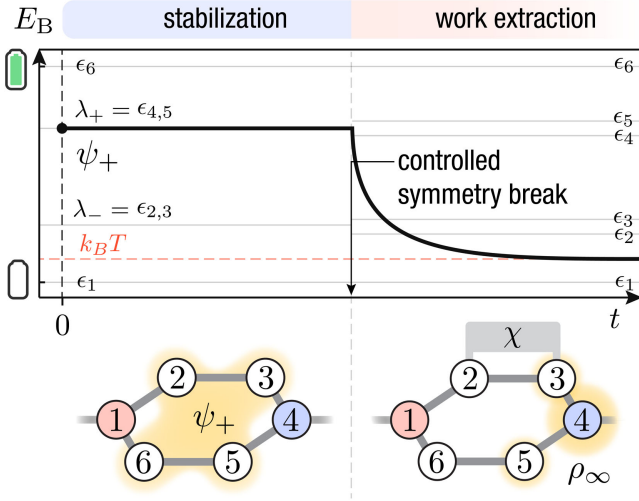


FIG. 9. Liu, Segal, and Hanna (2019) considered Eq. (59) with nearest-neighbor couplings J_{jk} with cyclic boundary conditions. The bulk sites $j = 2, 3, 5,$ and 6 are set with the same energy $E_j = E_{\text{bulk}}$, which differs from E_1 and E_4 . All couplings are chosen to be $J_{jk} = J_0$. The environment is coupled to the battery only via the surface site operators $\mathcal{S} = \{|1\rangle\langle 1|, |4\rangle\langle 4|\}$. The unitary operator $\hat{\Pi} = \exp[i(|2\rangle\langle 6| + \text{H.c.})] \exp[i(|3\rangle\langle 5| + \text{H.c.})]$ commutes with \mathcal{S} . This system has two DFSs associated with the eigenvalues $\lambda_{\pm} = E_{\text{bulk}} \pm J_0$ of Π and its eigenstates $|\psi_{\pm}\rangle = (1/2)(|6\rangle - |2\rangle \pm |5\rangle \mp |3\rangle)$. An initial charged state $|\psi_{+}\rangle$ can be preserved indefinitely. Work can be extracted by funneling energy to a target site ($j = 4$), thereby breaking the symmetry with small perturbations χ of the energy of the bulk sites.

environment (Liu, Segal, and Hanna, 2019). Second, charging the battery in such dark states is a challenging task in its own right. Sudden quenches, such as optical pumping with a pulsed laser, can take both the system and the environment out of equilibrium and generate correlations between strongly coupled excitons and phonons (Wells and Blank, 2008). Third, Liu’s proposal has been the subject of a discussion around its loss-free nature and ability to store energy (Liu, Segal, and Hanna, 2021; Tejero, Thingna, and Manzano, 2021) rather than just excitons. Nonetheless, the general consensus is that relaxation-free subspaces are a promising way to protect quantum batteries from energy losses and should be a subject of further study.

Further work is needed to generalize loss-free quantum batteries to the case of many-body systems. Another observation is that dark states like $|\psi_{\pm}\rangle$ are not the most energetic states of the battery Hamiltonian and instead sit roughly in the middle of its spectrum. This is akin to the subradiant states of Dicke models, which sit around the midpoint of the Dicke ladder (Glicenstein *et al.*, 2022). Therefore, it is important to understand whether there is a trade-off relation between the robustness of dark states and their energetic content, and whether they are compatible with superextensive power scaling. Future work should explore the possibility of using high-energy ratchet states¹⁷ while retaining absorption enhancement (Quach *et al.*, 2022).

¹⁷Excited states that can absorb but not emit light (Higgins, Lovett, and Gauger, 2017).

2. Engineering spontaneous dark-state preparation

Loss-free quantum batteries rely on our ability to prepare dark states. However, adiabatic passage and quantum optimal control may not always be viable options, due to limitations on the set of control operations and their bandwidth. Note that protected states can also form spontaneously due to an interaction with an auxiliary charger and the environment. This approach, which was proposed by Quach and Munro (2020), can be adopted to protect many-body excitonic quantum batteries from radiative and vibrational losses while retaining the superextensive scaling in the charging power discussed in Secs. II and III.

Quach and Munro (2020) considered an N_B -body battery and an N_C -body charger, both given by ensembles of uncoupled quantum TLSs with an energy gap ω . The battery and the charger are also coupled with a thermal reservoir, given by a bath of optical harmonic modes at a temperature T . The total system-reservoir Hamiltonian is

$$H = \omega(\hat{J}_B^z + \hat{J}_C^z) + \int dk E_k \hat{r}_k^\dagger \hat{r}_k + \frac{g}{2} [(\hat{J}_B^+ + \hat{J}_C^+) \hat{R} + (\hat{J}_B^- + \hat{J}_C^-) \hat{R}^\dagger], \quad (61)$$

where $\hat{J}_i^{x,y,z}$ denotes the usual collective spin operator of ensembles $i = B, C$ and $\hat{J}_i^\pm := \hat{J}_i^x \pm i\hat{J}_i^y$. The reservoir is represented via the linear dispersion relation E_k as a function of the wave vector \mathbf{k} with the creation and annihilation operators \hat{r}_k and \hat{r}_k^\dagger , respectively. The parameter g represents the coupling strength between the battery-charger system and the reservoir, while the reservoir operator $\hat{R} = \int dk \kappa_k \hat{r}_k$ is expressed as a function of a general continuous function κ_k whose form depends on the considered system. The reservoir is assumed to be weakly coupled ($g \ll \omega$) to the system and approximately in the thermal state $G_\beta[H_R] = \exp[-\beta H_R]/\mathcal{Z}$, with $H_R = \int dk E_k \hat{r}_k^\dagger \hat{r}_k$. Under these conditions, the dynamics of the system’s density operator $\rho(t)$ is well approximated via the Markovian GKSL master equation as

$$\dot{\rho}(t) = -i\omega[\hat{J}_B^z + \hat{J}_C^z, \rho(t)] + \gamma(\bar{n} + 1)\mathcal{D}_-[\rho] + \gamma\bar{n}\mathcal{D}_+[\rho], \quad (62)$$

where $\mathcal{D}_\pm[\rho] := 2\hat{O}\rho\hat{O}^\dagger - \{\hat{O}^\dagger\hat{O}, \rho\}$, with $\hat{O} = \hat{J}_B^\pm + \hat{J}_C^\pm$, γ a function of g , and $\bar{n} = 1/[\exp(\beta\omega) - 1]$ the mean thermal population.

Although the battery and charger are not directly coupled, the superoperators \mathcal{D}_\pm can generate correlations between the spins of the two subsystems. Quach and Munro (2020) considered an initial product state $|\psi_0\rangle = |G\rangle_B \otimes |E\rangle_C$ given by the ground state of the battery and the excited state of the charger. The dynamical map generated by Eq. (62) leads $|\psi_0\rangle$ to a steady state ρ_∞ that partially overlaps with a dark state forbidden from further decaying toward a completely passive thermal equilibrium state. Even at zero temperature this approach allows a battery state with finite energy to be prepared. With a numerical study conducted for $N_B \leq 10$, Quach and Munro (2020) showed that the power density scales linearly as $\langle P \rangle_\tau / N_B \propto N_B$, thus exceeding that of the Dicke model in the regime discussed in Sec. III.B.

Quantum *metastability*¹⁸ (Macieszczak *et al.*, 2016, 2021) may offer a path to the spontaneous formation of protected states, thus helping to develop approaches to mitigate energy loss in quantum batteries (Arjmandi *et al.*, 2022; Song *et al.*, 2022).

VI. EXPERIMENTAL IMPLEMENTATIONS

This section is devoted to the presentation of the most promising platforms for the realization of quantum batteries. We can broadly divide suitable platforms in two macrocategories: (i) platforms operating at ultralow temperatures and (ii) platforms that work at room temperature.

Regarding the first macrocategory, any platform for quantum computing is suitable for realizing quantum batteries. Examples of scalable solid-state Dicke batteries in the quantum coherent regime (Ferraro *et al.*, 2018) include semiconductor quantum dots (Burkard *et al.*, 2023) and superconducting materials (Blais *et al.*, 2021). Other alternatives include nitrogen-vacancy (NV) centers in diamond (Schirhagl *et al.*, 2014; Casola, van der Sar, and Yacoby, 2018; Barry *et al.*, 2020), neutral atoms, Rydberg atoms (Adams, Pritchard, and Shaffer, 2020), and trapped ions (Bruzewicz *et al.*, 2019). The realization of SYK quantum batteries is much more challenging in that no experimental system where the SYK model has been realized is yet available. However, potential candidates include graphene quantum dots with disordered edges subject to quantizing magnetic fields (Chen *et al.*, 2018; Brzezinska *et al.*, 2023) and strange metals (Patel and Sachdev, 2019; Hartnoll and Mackenzie, 2022) that are not well described by Landau's Fermi liquid theory.

First, battery platforms in the second macrocategory should contain quantum systems with level spacings ΔE that greatly exceed the room-temperature thermal energy $k_B T \approx 25$ meV to be sufficiently robust to energy relaxation. Second, they are expected to be dominated by a collective behavior rather than being based on entanglement generation (Cruz *et al.*, 2022) because the decoherence rate becomes faster as temperature increases.

A. Superconductors

Circuit QED setups (Blais *et al.*, 2021) offer the opportunity to simulate [in the sense of *quantum simulation* (Daley *et al.*, 2022)] some of the most important models of quantum optics. For example, the Tavis-Cummings (TC) model [recently studied for quantum batteries by Yang *et al.* (2024)], which describes a system of N TLSs coupled to a single-mode cavity, was simulated in a circuit QED setup by Fink *et al.* (2009). The TC model differs from the Dicke model in that it does not contain counterrotating terms. Circuit QED therefore offers us a natural platform to fabricate Dicke quantum batteries, as discussed in Sec. III.B. In such a platform, TLSs can be realized using superconducting qubits named transmons (Koch *et al.*, 2007), while the cavity is realized using a

coplanar waveguide resonator. The qubits are positioned at the antinodes of the first-harmonic standing wave electric field and have couplings that are nearly identical to the cavity mode. The resonators are typically realized by employing optical lithography and metal evaporation techniques on suitable substrates (Fink *et al.*, 2009), while the transmons are fabricated by combining e -beam lithography and shadow evaporation techniques for the metal of choice [typically aluminum, niobium, or, more recently, tantalum (Place *et al.*, 2021)] and its oxide. Recent developments on materials science aspects were addressed by Polini *et al.* (2022). Circuit QED setups are operated in the microwave regime (with typical level spacing being on the order of a few gigahertz) and display timescales on the order of nanoseconds.

A preliminary prototype of a superconducting quantum battery was realized experimentally by Hu *et al.* (2022). The device contained a single superconducting qutrit (i.e., a three-level system) coupled to a single-mode cavity. This system cannot display either a quantum or a collective advantage, since it contains a single quantum unit. The work of Hu *et al.*, however, constitutes an important first step toward realizing highly controllable superconducting quantum devices capable of storing energy. Indeed, using two microwave pulses with time-dependent Rabi frequencies, Hu *et al.* (2022) were able to resonantly drive the qutrit and implement a number of controlled adiabatic charging processes, such as those discussed in Sec. IV.B. Superconducting implementations can also be studied, with some limitations, on platforms like the IBM Quantum Experience (Gemme *et al.*, 2022).

B. Quantum dots

Wenniger *et al.* (2022) conducted an experimental study of energy transfer between a TLS and a reservoir of electromagnetic modes. The energy transfer occurred via spontaneous emission from a InGaAs quantum dot (the charger) to a micropillar optical cavity (the battery). The quantum dot was resonantly excited by a pulsed Ti:sapphire laser in a cryostat at 5–20 K, to be brought into a superposition of the ground and excited states. Wenniger *et al.* (2022) also considered a work extraction phase during which the energy stored in the battery flowed into another system (a laser field) through homodyne-type interference. After spontaneous emission of the quantum dot into the cavity, the work transferred to the battery corresponded to the coherent part of the emitted field, while the incoherent component corresponded to the heat exchanged. The latter was an energy-loss mechanism and did not contribute to work extraction. Further efforts could employ this setup with many-body quantum batteries and approaches to protect active states from relaxation.

C. Organic microcavities

Quach *et al.* (2022) presented an experimental implementation of a many-body charging protocol, realized using an organic semiconductor coupled to a confined optical mode in a microcavity at room temperature. They provided evidence for the system displaying superextensive scaling of the energy absorption while interpreting the results in terms of the Dicke model discussed in Sec. III.B. The setup consisted of a

¹⁸In quantum metastability, which is related to prethermalization (Berges, Borsányi, and Wetterich, 2004), relaxation rapidly leads the system toward long-lived nonequilibrium states, from which thermal equilibration is reached over exponentially longer timescales.

microcavity formed of two dielectric mirrors (Vahala, 2003) containing a thin layer of a low-mass molecular semiconductor [Lumogen F Orange (LFO) (Russo *et al.*, 2022)] dispersed in a polymer matrix. Operating around the 0-0 transition,¹⁹ the LFO molecules can be considered as TLSs, supporting the use of the Dicke model. The number of TLSs was varied by controlling the concentrations of the dye molecules. Moreover, charging and energy storage dynamics were measured using ultrafast transient-absorption spectroscopy, allowing femtosecond charging times to be measured (Cerullo *et al.*, 2007). Quach *et al.* (2022) observed that the retention of energy in the system had the benefit of a finely tuned balance between cavity coupling and decoherence channels, allowing the device to charge quickly and yet discharge much more slowly. This effect, which is analogous to that discussed in Sec. V.C, provides an example of a realistic noisy environment that can aid in the implementation of quantum batteries.

A practical challenge discussed by Quach *et al.* (2022) was that high concentrations of dye molecules led to quenching, i.e., the formation of optically dark electronic ground states that suppress light absorption. Overcoming this limitation would require a careful choice of materials, so as to mitigate or eliminate quenching. There are classes of materials where such quenching is suppressed. For example, fluorescent molecules can be surrounded by a “molecular cage” or “bumper,” for example, one consisting of protein β sheets (Dietrich *et al.*, 2016). These cages force a minimum distance between the chromophores that reduces the intermolecular electronic couplings, thus allowing for the suppression of exciton-exciton quenching at high concentrations (Dietrich *et al.*, 2016). Such materials are a promising route to studying quantum battery at higher molecular concentrations and higher energy densities.

D. Nuclear spins

Joshi and Mahesh (2022) recently used nuclear magnetic resonance to study energy injection and extraction in nuclear spin systems. They considered molecular structures with star topology consisting of a so-called battery spin surrounded by $\mathcal{N} = 3$ to 36 charger spins. They employed a single spin-1/2 battery, and the charger was a collection of \mathcal{N} spin-1/2 systems. Although these systems resemble the spin-network models discussed in Sec. III.C.1, here the “battery” is a single-body system ($N = 1$), while the charger is composed of $\mathcal{N} > 1$ subunits. The experiments were conducted at an ambient temperature of 298 K. The initial thermal equilibrium state of the charger spins were driven out of equilibrium by inverting their populations with a π pulse. The energy of the battery spin was then measured as a function of time and of the number \mathcal{N} of the charger spins. Although similar in nature, the charging speedup measured by Joshi and Mahesh (2022) is not exactly the one described in Sec. II [the battery is indeed composed of a single constituent ($N = 1$)] but rather a case of the *supertransfer* mechanism (Taylor and Kassal, 2018).

In the full 38-spin system of Joshi and Mahesh (2022), the battery could store energy for up to 2 min. This result is a promising step toward the implementation of room-temperature quantum batteries based on nuclear spins. Further work could extend this model to the case of many-body quantum batteries (i.e., $N > 1$) and could clarify the nature of the charging speedup scaling with \mathcal{N} .

VII. CONCLUSIONS AND OUTLOOK

In the past decade, quantum batteries have been a framework for studying energy injection, storage, and extraction processes in the quantum regime. Despite significant progress, we are only now beginning to understand the potential and the applications of quantum energy storage. A complication is posed by the fact that batteries are multifaceted devices whose performance is evaluated using a variety of figures of merit. Therefore, we could argue that a quantum battery is well defined only with a clear goal in mind. Hence, the following question is of paramount importance: What are the uses for a quantum battery? Here we outline a few possible answers while elaborating on how they could set a path for future developments.

One option is to focus on the advantages that quantum batteries may offer over classical ones. At the beginning of this Colloquium we set out to determine whether genuine quantum effects can improve the performance of energy storage devices. The results that we reviewed suggest that the answer is in the affirmative, as discussed in Secs. II and III, at least in some systems and under conditions intended to preserve such key quantum features.

Another avenue for quantum batteries is their integration into emerging quantum technologies, which are expected to assume a prominent role in a variety of practical tasks (Acín *et al.*, 2018; Deutsch, 2020), such as optimizations (Preskill, 2018; Atzori and Sessoli, 2019), simulations (Altman *et al.*, 2021), and measurements (Degen, Reinhard, and Cappellaro, 2017; Albarelli *et al.*, 2020). As a major example, quantum computation necessitates examining its energy consumption for practical implementation and optimization (Auffèves, 2022). Bennett (1973) connected logical reversibility in computation to thermodynamic reversibility, suggesting no heat generation in logically reversible computations that prevent information loss, which adheres to Landauer’s principle (Landauer, 1961). Quantum computation is inherently reversible because it uses unitary operations. This feature allows, at least in theory, quantum computation to be performed without generating heat. However, owing to the quantum speed limit (Deffner and Campbell, 2017) finite-time operations require energy input, necessitating an energy source for a reversible quantum computer, even without heat production.

Chiribella, Yang, and Renner (2021) demonstrated the necessity of a quantum energy storage component when performing reversible quantum computing. Their proposed approach involves implementing a reversible quantum gate G , which might not conserve energy, on the system used for the computation through a free unitary U_G . The latter acts on both the system and the battery by preserving their combined energy. Ideally the battery needs to supply only a finite energy

¹⁹In the presence of vibrational sublevels, 0-0 transitions are those between the lowest vibrational states.

for U_G to approximate the desired gate G with arbitrary precision. Chiribella, Yang, and Renner (2021) discussed the energetic requirements for reversible quantum computing in relation to those imposed by Landauer’s principle for irreversible processes. These results speak to the importance that quantum batteries have for energy-efficient computing, encouraging the investigation of several aspects, such as the relation to the quantum speed limit (Deffner and Campbell, 2017) and the finite-time Landauer principle (Proesmans, Ehrich, and Bechhoefer, 2020).

Beyond computation, quantum batteries could prove resourceful for other quantum devices that rely on coherences and entanglement. The scheme proposed by Chiribella, Yang, and Renner (2021) also finds an application in quantum metrology (Chiribella and Yang, 2017) and has general validity for reversible quantum operations. In this context, it is likely that the energy storage components would require some unique conditions to correctly interface with some quantum device. For example, batteries might need to operate at energy scales and timescales that can be achieved only with, say, transmons, just as superconducting quantum interference devices and NV centers are among the few available platforms to offer nanotesla sensitivity for magnetometry (Buchner *et al.*, 2018; Barry *et al.*, 2020). Based on these perspectives, we can outline a road map for the development of quantum batteries. In what follows, we start with theory and proceed through experiments to arrive at future possible applications.

A key theoretical question is to understand whether the amount of extractable energy affects the relaxation timescale. Decoherence-free subspaces (Kwiat *et al.*, 2000; Lidar and Birgitta Whaley, 2003; Cappellaro *et al.*, 2006), metastability (see Sec. V.C.1) (Lan *et al.*, 2018; Macieszczak *et al.*, 2021), and anomalous relaxation (Lu and Raz, 2017; Baity-Jesi *et al.*, 2019; Carollo, Lasanta, and Lesanovsky, 2021; Wildeboer, Iadecola, and Williamson, 2022) offer a viable way to overcome the trade-off that is apparently imposed by the relaxation rate $\gamma_R \propto \exp(\Delta E/k_B T)$, which is exponentially faster with an increasing energy gap ΔE . We need to find models that permit these phenomena and platforms to realize them. Studying the limits of energy density of quantum battery architectures is another opportunity to push the field beyond power scaling. Proof-of-principle experiments are the next step in demonstrating advantages and uncovering new aspects of quantum energy storage. With the experimental work on quantum batteries still in its infancy, it is desirable to consider all existing platforms for quantum technologies (Smyser and Eaves, 2020; de Leon *et al.*, 2021; Huang *et al.*, 2023).

Finally, we consider the relation between the previously discussed physical architectures and applications. The distinction between quantum and collective effects (see Secs. II and III) suggests that “cold” platforms would be ideal to explore quantum speedups. This is because most of the experimental setups that can sustain entanglement work at low temperatures. These conditions are achieved using cryostats and other energy-consuming controls; therefore, we must also carefully account for the associated energy expenditure (Auffèves, 2022; Fellous-Asiani *et al.*, 2023). However, room-temperature setups offer a path toward collective speedups. Architectures based on quantum dots and organic molecules are strong candidates due to energy densities that are favorable

for optoelectronics (Ostroverkhova, 2016) and have already found an application in light-harvesting devices (Calvin, 1983; Curutchet and Mennucci, 2017; Kundu and Patra, 2017; Jang and Mennucci, 2018).

In conclusion, for quantum batteries to make a direct technological impact, we must address the aforementioned important issues, like stabilization efficiency and energy density. Note that this Colloquium does not address the use of genuine quantum effects to enhance existing energy technologies like electrochemical batteries, capacitors, and solar cells. This is a promising and relatively underexplored direction, with few exceptions, such as quantum supercapacitors (Ferraro *et al.*, 2019) and the role of coherence in light harvesting (Scully, 2010; Kaake, Moses, and Heeger, 2013; Chenu and Scholes, 2015; Brédas, Sargent, and Scholes, 2017; Curutchet and Mennucci, 2017; Jang and Mennucci, 2018).

The management of energy resources is a key topic in social and political discussions. Surprisingly, quantum technology research has only recently begun to address this issue (Auffèves, 2022). Recent findings suggest that quantum technologies can revolutionize energy harvesting (Curutchet and Mennucci, 2017; Wang *et al.*, 2018), storage (Ho, McClean, and Ong, 2018; Gao *et al.*, 2021), delivery (Zhong *et al.*, 2016; Mattioni *et al.*, 2021; Davidson, Pollock, and Gauger, 2022), and conversion (von Lindenfels *et al.*, 2019; Ono *et al.*, 2020), thereby giving rise to a quantum energy sector (Metzler, Sandoval, and Galvanetto, 2023). Scientific revolutions often arise from basic research, and quantum batteries play a crucial role in advancing our fundamental understanding of energy storage.

ACKNOWLEDGMENTS

We thank Professor Kavan Modi for the insightful discussions. We also acknowledge the valuable feedback provided by A. Auffèves, F. Binder, M. Carrega, A. Crescente, S. Deffner, F. Q. Dou, D. Ferraro, V. Giovannetti, S. Julià-Farré, D. Rosa, D. Rossini, and A. C. Santos. F. C. acknowledges that results incorporated in this standard have received funding from the European Union Horizon Europe research and innovation program under the Marie Skłodowska-Curie Action for the project SpinSC. S. G. acknowledges the European Commission under Grant Agreement No. 101070546 (MUQUABIS), PNRR MUR Project No. PE0000023-NQSTI funded by the European Union—Next Generation EU, and Royal Society Grant No. IEC \R2\222003. G. M. A. acknowledges funding from the European Research Council (ERC) under the European Union’s Horizon 2020 research and innovation program [Grant Agreement No. 101002955 (CONQUER)].

M. P. is a cofounder and shareholder of Planckian. All other authors declare no competing interests.

REFERENCES

- Abah, O., G. De Chiara, M. Paternostro, and R. Puebla, 2022, *Phys. Rev. Res.* **4**, L022017.
- Acín, A., *et al.*, 2018, *New J. Phys.* **20**, 080201.
- Adams, C. S., J. D. Pritchard, and J. P. Shaffer, 2020, *J. Phys. B* **53**, 012002.

- Albarelli, F., M. Barbieri, M. Genoni, and I. Gianani, 2020, *Phys. Lett. A* **384**, 126311.
- Alicki, R., 2019, *J. Chem. Phys.* **150**, 214110.
- Alicki, R., and M. Fannes, 2013, *Phys. Rev. E* **87**, 042123.
- Allahverdyan, A. E., R. Balian, and T. M. Nieuwenhuizen, 2004, *Europhys. Lett.* **67**, 565.
- Altman, E., *et al.*, 2021, *PRX Quantum* **2**, 017003.
- Andolina, G. M., 2020, Ph.D. thesis (Scuola Normale Superiore).
- Andolina, G. M., D. Farina, A. Mari, V. Pellegrini, V. Giovannetti, and M. Polini, 2018, *Phys. Rev. B* **98**, 205423.
- Andolina, G. M., M. Keck, A. Mari, M. Campisi, V. Giovannetti, and M. Polini, 2019, *Phys. Rev. Lett.* **122**, 047702.
- Andolina, G. M., M. Keck, A. Mari, V. Giovannetti, and M. Polini, 2019, *Phys. Rev. B* **99**, 205437.
- Angerer, A., *et al.*, 2018, *Nat. Phys.* **14**, 1168.
- Arjmandi, M. B., H. Mohammadi, and A. C. Santos, 2022, *Phys. Rev. E* **105**, 054115.
- Arjmandi, M. B., A. Shokri, E. Faizi, and H. Mohammadi, 2022, *Phys. Rev. A* **106**, 062609.
- Atzori, M., and R. Sessoli, 2019, *J. Am. Chem. Soc.* **141**, 11339.
- Aubrun, G., and S. J. Szarek, 2006, *Phys. Rev. A* **73**, 022109.
- Auerbach, A., 1994, *Interacting Electrons, and Quantum Magnetism* (Springer, New York).
- Auffèves, A., 2022, *PRX Quantum* **3**, 020101.
- Bacon, D., J. Kempe, D. A. Lidar, and K. B. Whaley, 2000, *Phys. Rev. Lett.* **85**, 1758.
- Bai, S. Y., and J. H. An, 2020, *Phys. Rev. A* **102**, 060201(R).
- Baity-Jesi, M., *et al.*, 2019, *Proc. Natl. Acad. Sci. U.S.A.* **116**, 15350.
- Bakhshinezhad, F., B. R. Jabloński, F. C. Binder, and N. Friis, 2024, *Phys. Rev. E* **109**, 014131.
- Bancewicz, M., G. H. F. Diercksen, and J. Karwowski, 1989, *Phys. Rev. A* **40**, 5507.
- Barndorff-Nielsen, O. E., and R. D. Gill, 2000, *J. Phys. A* **33**, 4481.
- Barra, F., 2019, *Phys. Rev. Lett.* **122**, 210601.
- Barra, F., 2022, *Entropy* **24**, 820.
- Barra, F., K. V. Hovhannisyán, and A. Imperato, 2022, *New J. Phys.* **24**, 015003.
- Barra, F., and C. Lledó, 2017, *Phys. Rev. E* **96**, 052114.
- Barry, J. F., J. M. Schloss, E. Bauch, M. J. Turner, C. A. Hart, L. M. Pham, and R. L. Walsworth, 2020, *Rev. Mod. Phys.* **92**, 015004.
- Batalhão, T. B., S. Gherardini, J. P. Santos, G. T. Landi, and M. Paternostro, 2019, in *Lectures on Quantum Computing, Thermodynamics and Statistical Physics* (Springer, Cham, Switzerland), pp. 395–410.
- Baumann, K., C. Guerlin, F. Brennecke, and T. Esslinger, 2010, *Nature (London)* **464**, 1301.
- Beige, A., D. Braun, B. Tregenna, and P. L. Knight, 2000, *Phys. Rev. Lett.* **85**, 1762.
- Belavkin, V., 1987, in *Information Complexity and Control in Quantum Physics* (Springer, New York), pp. 311–329.
- Bennett, C. H., 1973, *IBM J. Res. Dev.* **17**, 525.
- Berges, J., S. Borsányi, and C. Wetterich, 2004, *Phys. Rev. Lett.* **93**, 142002.
- Berry, M. V., 2009, *J. Phys. A* **42**, 365303.
- Bérut, A., A. Arakelyan, A. Petrosyan, S. Ciliberto, R. Dillenschneider, and E. Lutz, 2012, *Nature (London)* **483**, 187.
- Bianchi, E., L. Hackl, M. Kieburg, M. Rigol, and L. Vidmar, 2022, *PRX Quantum* **3**, 030201.
- Binder, F., L. A. Correa, C. Gogolin, J. Anders, and G. Adesso, 2018, Eds., *Thermodynamics in the Quantum Regime*, Fundamental Theories of Physics Vol. 195 (Springer International Publishing, Cham, Switzerland).
- Binder, F., S. Vinjanampathy, K. Modi, and J. Goold, 2015a, *Phys. Rev. E* **91**, 032119.
- Binder, F. C., S. Vinjanampathy, K. Modi, and J. Goold, 2015b, *New J. Phys.* **17**, 075015.
- Blais, A., A. L. Grimsmo, S. M. Girvin, and A. Wallraff, 2021, *Rev. Mod. Phys.* **93**, 025005.
- Braak, D., 2011, *Phys. Rev. Lett.* **107**, 100401.
- Brédas, J. L., E. H. Sargent, and G. D. Scholes, 2017, *Nat. Mater.* **16**, 35.
- Breuer, H.-P., and F. Petruccione, 2002, *The Theory of Open Quantum Systems* (Oxford University Press, New York).
- Brunner, N., N. Linden, S. Popescu, and P. Skrzypczyk, 2012, *Phys. Rev. E* **85**, 051117.
- Bruzewicz, C. D., J. Chiaverini, R. McConnell, and J. M. Sage, 2019, *Appl. Phys. Rev.* **6**, 021314.
- Brzezinska, M., Y. Guan, O. V. Yazyev, S. Sachdev, and A. Kruchkov, 2023, *Phys. Rev. Lett.* **131**, 036503.
- Buchner, M., K. Höfler, B. Henne, V. Ney, and A. Ney, 2018, *J. Appl. Phys.* **124**, 161101.
- Burkard, G., T. D. Ladd, J. M. Nichol, A. Pan, and J. R. Petta, 2023, *Rev. Mod. Phys.* **95**, 025003.
- Calvin, M., 1983, *Photochem. Photobiol.* **37**, 349.
- Camati, P. A., J. P. S. Peterson, T. B. Batalhão, K. Micadei, A. M. Souza, R. S. Sarthour, I. S. Oliveira, and R. M. Serra, 2016, *Phys. Rev. Lett.* **117**, 240502.
- Campaioli, F., 2020, Ph.D. thesis (Monash University), https://bridges.monash.edu/articles/thesis/Tightening_Time-Energy_Uncertainty_Relations/11833566.
- Campaioli, F., F. Pollock, F. Binder, L. Céleri, J. Goold, S. Vinjanampathy, and K. Modi, 2017, *Phys. Rev. Lett.* **118**, 150601.
- Campaioli, F., W. Sloan, K. Modi, and F. A. Pollock, 2019, *Phys. Rev. A* **100**, 062328.
- Campbell, S., and S. Deffner, 2017, *Phys. Rev. Lett.* **118**, 100601.
- Caneva, T., T. Calarco, and S. Montangero, 2012, *New J. Phys.* **14**, 093041.
- Cappellaro, P., J. S. Hodges, T. F. Havel, and D. G. Cory, 2006, *J. Chem. Phys.* **125**, 044514.
- Caravelli, F., G. Coulter-De Wit, L. P. García-Pintos, and A. Hamma, 2020, *Phys. Rev. Res.* **2**, 023095.
- Caravelli, F., B. Yan, L. P. García-Pintos, and A. Hamma, 2021, *Quantum* **5**, 505.
- Carnot, S., 1824, *Reflections on the Motive Power of Fire* (Paris).
- Carollo, F., A. Lasanta, and I. Lesanovsky, 2021, *Phys. Rev. Lett.* **127**, 060401.
- Carrasco, J., J. R. Maze, C. Hermann-Avigliano, and F. Barra, 2022, *Phys. Rev. E* **105**, 064119.
- Carrega, M., A. Crescente, D. Ferraro, and M. Sassetti, 2020, *New J. Phys.* **22**, 083085.
- Casola, F., T. van der Sar, and A. Yacoby, 2018, *Nat. Rev. Mater.* **3**, 17088.
- Centrone, F., L. Mancino, and M. Paternostro, 2023, *Phys. Rev. A* **108**, 052213.
- Cerullo, G., C. Manzoni, L. Lüer, and D. Polli, 2007, *Photochem. Photobiol. Sci.* **6**, 135.
- Chaki, P., A. Bhattacharyya, K. Sen, and U. Sen, 2023, [arXiv:2307.16856](https://arxiv.org/abs/2307.16856).
- Chang, W., T. R. Yang, H. Dong, L. Fu, X. Wang, and Y. Y. Zhang, 2021, *New J. Phys.* **23**, 103026.
- Chávez-Carlos, J., B. López-del Carpio, M. A. Bastarrachea-Magnani, P. Stránský, S. Lerma-Hernández, L. F. Santos, and J. G. Hirsch, 2019, *Phys. Rev. Lett.* **122**, 024101.
- Chen, A., R. Ilan, F. de Juan, D. I. Pikulin, and M. Franz, 2018, *Phys. Rev. Lett.* **121**, 036403.

- Chen, P., T. S. Yin, Z. Q. Jiang, and G. R. Jin, 2022, *Phys. Rev. E* **106**, 054119.
- Chenu, A., and G. D. Scholes, 2015, *Annu. Rev. Phys. Chem.* **66**, 69.
- Chiara, G. D., G. Landi, A. Hewgill, B. Reid, A. Ferraro, A. J. Roncaglia, and M. Antezza, 2018, *New J. Phys.* **20**, 113024.
- Chiribella, G., and Y. Yang, 2017, *Phys. Rev. A* **96**, 022327.
- Chiribella, G., Y. Yang, and R. Renner, 2021, *Phys. Rev. X* **11**, 021014.
- Chruściński, D., and S. Pascazio, 2017, *Open Syst. Inf. Dyn.* **24**, 1740001.
- Ciccarello, F., S. Lorenzo, V. Giovannetti, and G. M. Palma, 2022, *Phys. Rep.* **954**, 1.
- Crescente, A., M. Carrega, M. Sassetti, and D. Ferraro, 2020a, *Phys. Rev. B* **102**, 245407.
- Crescente, A., M. Carrega, M. Sassetti, and D. Ferraro, 2020b, *New J. Phys.* **22**, 063057.
- Crescente, A., D. Ferraro, M. Carrega, and M. Sassetti, 2022, *Phys. Rev. Res.* **4**, 033216.
- Crescente, A., D. Ferraro, M. Carrega, and M. Sassetti, 2023, *Entropy*, **25**, 758.
- Cruz, C., M. F. Anka, M. S. Reis, R. Bachelard, and A. C. Santos, 2022, *Quantum Sci. Technol.* **7**, 025020.
- Curutchet, C., and B. Mennucci, 2017, *Chem. Rev.* **117**, 294.
- Daley, A. J., I. Bloch, C. Kokail, S. Flannigan, N. Pearson, M. Troyer, and P. Zoller, 2022, *Nature (London)* **607**, 667.
- Davidson, S., F. A. Pollock, and E. Gauger, 2022, *PRX Quantum* **3**, 020354.
- de Aguiar, M., K. Furuya, C. Lewenkopf, and M. Nemes, 1992, *Ann. Phys. (N.Y.)* **216**, 291.
- Deffner, S., and S. Campbell, 2017, *J. Phys. A* **50**, 453001.
- Deffner, S., and E. Lutz, 2013, *J. Phys. A* **46**, 335302.
- Degen, C. L., F. Reinhard, and P. Cappellaro, 2017, *Rev. Mod. Phys.* **89**, 035002.
- de Leon, N. P., K. M. Itoh, D. Kim, K. K. Mehta, T. E. Northup, H. Paik, B. S. Palmer, N. Samarth, S. Sangtawesin, and D. W. Steuerman, 2021, *Science* **372**, eabb2823.
- Delmonte, A., A. Crescente, M. Carrega, D. Ferraro, and M. Sassetti, 2021, *Entropy*, **23**, 612.
- de Ponte, M., S. Mizrahi, and M. Moussa, 2007, *Ann. Phys. (N.Y.)* **322**, 2077.
- Deutsch, I. H., 2020, *PRX Quantum* **1**, 020101.
- Dicke, R. H., 1954, *Phys. Rev.* **93**, 99.
- Dietrich, C. P., A. Steude, L. Tropic, M. Schubert, N. M. Kronenberg, K. Ostermann, S. Hofling, and M. C. Gather, 2016, *Sci. Adv.* **2**, e1600666.
- Dou, F.-Q., Y.-Q. Lu, Y.-J. Wang, and J.-A. Sun, 2022, *Phys. Rev. B* **105**, 115405.
- Dou, F.-Q., Y. J. Wang, and J. A. Sun, 2020, *Europhys. Lett.* **131**, 43001.
- Dou, F.-Q., Y. J. Wang, and J. A. Sun, 2022a, *Front. Phys.* **17**, 31503.
- Dou, F.-Q., Y.-J. Wang, and J.-A. Sun, 2022b, *arXiv:2208.04831*.
- Dou, F.-Q., and F.-M. Yang, 2023, *Phys. Rev. A* **107**, 023725.
- Dou, F.-Q., H. Zhou, and J.-A. Sun, 2022, *Phys. Rev. A* **106**, 032212.
- Fan, J., S. Wu, and C.-s. Yu, 2021, *Quantum Inf. Process.* **20**, 9.
- Farina, D., G. M. Andolina, A. Mari, M. Polini, and V. Giovannetti, 2019, *Phys. Rev. B* **99**, 035421.
- Fedorov, A. K., N. Gisin, S. M. Belousov, and A. I. Lvovsky, 2022, *arXiv:2203.17181*.
- Felicetti, S., J. S. Pedernales, I. L. Egusquiza, G. Romero, L. Lamata, D. Braak, and E. Solano, 2015, *Phys. Rev. A* **92**, 033817.
- Felicetti, S., D. Z. Rossatto, E. Rico, E. Solano, and P. Forn-Díaz, 2018, *Phys. Rev. A* **97**, 013851.
- Fellous-Asiani, M., J. H. Chai, Y. Thonnart, K. Ng, R. S. Whitney, and A. Auffèves, 2023, *PRX Quantum* **4**, 040319.
- Fermi, E., 1956, *Thermodynamics* (Dover, New York).
- Ferraro, D., G. M. Andolina, M. Campisi, V. Pellegrini, and M. Polini, 2019, *Phys. Rev. B* **100**, 075433.
- Ferraro, D., M. Campisi, G. M. Andolina, V. Pellegrini, and M. Polini, 2018, *Phys. Rev. Lett.* **120**, 117702.
- Fink, J. M., R. Bianchetti, M. Baur, M. Göppl, L. Steffen, S. Filipp, P. J. Leek, A. Blais, and A. Wallraff, 2009, *Phys. Rev. Lett.* **103**, 083601.
- Francica, G., F. C. Binder, G. Guarnieri, M. T. Mitchison, J. Goold, and F. Plastina, 2020, *Phys. Rev. Lett.* **125**, 180603.
- Friis, N., and M. Huber, 2018, *Quantum* **2**, 61.
- Fusco, L., M. Paternostro, and G. De Chiara, 2016, *Phys. Rev. E* **94**, 052122.
- Gao, L., C. Cheng, W.-B. He, R. Mondaini, X.-W. Guan, and H.-Q. Lin, 2022, *Phys. Rev. Res.* **4**, 043150.
- Gao, Q., H. Nakamura, T. P. Gujarati, G. O. Jones, J. E. Rice, S. P. Wood, M. Pistoia, J. M. Garcia, and N. Yamamoto, 2021, *J. Phys. Chem. A* **125**, 1827.
- Garbe, L., I. L. Egusquiza, E. Solano, C. Ciuti, T. Coudreau, P. Milman, and S. Felicetti, 2017, *Phys. Rev. A* **95**, 053854.
- Garbe, L., P. Wade, F. Minganti, N. Shammah, S. Felicetti, and F. Nori, 2020, *Sci. Rep.* **10**, 13408.
- Gardiner, C. W., and P. Zoller, 2000, *Quantum Noise* (Springer, New York).
- Gaubatz, U., P. Rudecki, S. Schiemann, and K. Bergmann, 1990, *J. Chem. Phys.* **92**, 5363.
- Gemme, G., G. M. Andolina, F. M. D. Pellegrino, M. Sassetti, and D. Ferraro, 2023, *Batteries* **9**, 197.
- Gemme, G., M. Grossi, D. Ferraro, S. Vallecorsa, and M. Sassetti, 2022, *Batteries* **8**, 43.
- Georges, A., O. Parcollet, and S. Sachdev, 2001, *Phys. Rev. B* **63**, 134406.
- Gherardini, S., 2019, *Phys. Rev. A* **99**, 062105.
- Gherardini, S., F. Campaioli, F. Caruso, and F. C. Binder, 2020, *Phys. Rev. Res.* **2**, 013095.
- Gherardini, S., G. Giachetti, S. Ruffo, and A. Trombettoni, 2021, *Phys. Rev. E* **104**, 034114.
- Gherardini, S., S. Gupta, F. S. Cataliotti, A. Smerzi, F. Caruso, and S. Ruffo, 2016, *New J. Phys.* **18**, 013048.
- Ghosh, S., T. Chanda, S. Mal, and A. Sen(De), 2021, *Phys. Rev. A* **104**, 032207.
- Ghosh, S., T. Chanda, and A. Sende, 2020, *Phys. Rev. A* **101**, 032115.
- Ghosh, S., and A. S. De, 2022, *Phys. Rev. A* **105**, 022628.
- Giorgi, G. L., and S. Campbell, 2015, *J. Phys. B* **48**, 035501.
- Giovannetti, V., S. Lloyd, and L. Maccone, 2003, *Phys. Rev. A* **67**, 052109.
- Giovannetti, V., S. Lloyd, and L. Maccone, 2011, *Nat. Photonics* **5**, 222.
- Gisin, N., G. Ribordy, W. Tittel, and H. Zbinden, 2002, *Rev. Mod. Phys.* **74**, 145.
- Glicenstein, A., G. Ferioli, A. Browaeys, and I. Ferrier-Barbut, 2022, *Opt. Lett.* **47**, 1541.
- Gross, M., and S. Haroche, 1982, *Phys. Rep.* **93**, 301.
- Guarnieri, G., D. Morrone, B. Çakmak, F. Plastina, and S. Campbell, 2020, *Phys. Lett. A* **384**, 126576.
- Guo, W.-X., F.-M. Yang, and F.-Q. Dou, 2024, *Phys. Rev. A* **109**, 032201.
- Gurvits, L., and H. Barnum, 2005, *Phys. Rev. A* **72**, 032322.
- Gyhm, J.-Y., D. Šafránek, and D. Rosa, 2022, *Phys. Rev. Lett.* **128**, 140501.
- Haroche, S., 2013, *Rev. Mod. Phys.* **85**, 1083.

- Hartnoll, S. A., and A. P. Mackenzie, 2022, *Rev. Mod. Phys.* **94**, 041002.
- Hepp, K., and E. Lieb, 1973, *Ann. Phys. (N.Y.)* **76**, 360.
- Hernández-Gómez, S., S. Gherardini, N. Staudenmaier, F. Poggiali, M. Campisi, A. Trombettoni, F. Cataliotti, P. Cappellaro, and N. Fabbri, 2022, *PRX Quantum* **3**, 020329.
- Higgins, K. D., B. W. Lovett, and E. M. Gauger, 2017, *J. Phys. Chem. C* **121**, 20714.
- Higgins, K. D. B., S. C. Benjamin, T. M. Stace, G. J. Milburn, B. W. Lovett, and E. M. Gauger, 2014, *Nat. Commun.* **5**, 4705.
- Ho, A., J. McClean, and S. P. Ong, 2018, *Joule* **2**, 810.
- Horodecki, R., P. Horodecki, M. Horodecki, and K. Horodecki, 2009, *Rev. Mod. Phys.* **81**, 865.
- Horowitz, J. M., and K. Jacobs, 2015, *Phys. Rev. Lett.* **115**, 130501.
- Hovhannisyán, K. V., F. Barra, and A. Imparato, 2020, *Phys. Rev. Res.*, **2**, 033413.
- Hovhannisyán, K. V., M. Perarnau-Llobet, M. Huber, and A. Acín, 2013, *Phys. Rev. Lett.* **111**, 240401.
- Hu, C.-K., *et al.*, 2022, *Quantum Sci. Technol.* **7**, 045018.
- Huang, X., K. Wang, L. Xiao, L. Gao, H. Lin, and P. Xue, 2023, *Phys. Rev. A* **107**, L030201.
- Huangfu, Y., and J. Jing, 2021, *Phys. Rev. E* **104**, 024129.
- Imai, S., O. Gühne, and S. Nimmrichter, 2023, *Phys. Rev. A* **107**, 022215.
- Jang, S. J., and B. Mennucci, 2018, *Rev. Mod. Phys.* **90**, 035003.
- Joshi, J., and T. S. Mahesh, 2022, *Phys. Rev. A* **106**, 042601.
- Julià-Farré, S., T. Salamon, A. Riera, M. N. Bera, and M. Lewenstein, 2020, *Phys. Rev. Res.* **2**, 023113.
- Kaake, L. G., D. Moses, and A. J. Heeger, 2013, *J. Phys. Chem. Lett.* **4**, 2264.
- Kaluzny, Y., P. Goy, M. Gross, J. M. Raimond, and S. Haroche, 1983, *Phys. Rev. Lett.* **51**, 1175.
- Kamin, F., F. Tabesh, S. Salimi, F. Kheirandish, and A. Santos, 2020, *New J. Phys.* **22**, 083037.
- Kamin, F. H., Z. Abuali, H. Ness, and S. Salimi, 2023, *J. Phys. A* **56**, 275302.
- Kamin, F. H., F. T. Tabesh, S. Salimi, and A. C. Santos, 2020, *Phys. Rev. E* **102**, 052109.
- Kieu, T. D., 2004, *Phys. Rev. Lett.* **93**, 140403.
- Kim, J., J. Murugan, J. Olle, and D. Rosa, 2022, *Phys. Rev. A* **105**, L010201.
- Kitaev, A., 2015, lecture, Kavli Institute for Theoretical Physics, University of California, Santa Barbara, <https://online.kitp.ucsb.edu/online/entangled15/kitaev/>.
- Kjäll, J. A., J. H. Bardarson, and F. Pollmann, 2014, *Phys. Rev. Lett.* **113**, 107204.
- Koch, J., T. M. Yu, J. Gambetta, A. A. Houck, D. I. Schuster, J. Majer, A. Blais, M. H. Devoret, S. M. Girvin, and R. J. Schoelkopf, 2007, *Phys. Rev. A* **76**, 042319.
- Konar, T. K., L. G. C. Lakkaraju, S. Ghosh, and A. S. De 2022, *Phys. Rev. A* **106**, 022618.
- Konar, T. K., A. Patra, R. Gupta, S. Ghosh, and A. S. De, 2022, *arXiv:2210.16528*.
- Kundu, S., and A. Patra, 2017, *Chem. Rev.* **117**, 712.
- Kwiat, P. G., A. J. Berglund, J. B. Altepeter, and A. G. White, 2000, *Science* **290**, 498.
- Ladd, T. D., F. Jelezko, R. Laflamme, Y. Nakamura, C. Monroe, and J. L. O'Brien, 2010, *Nature (London)* **464**, 45.
- Lan, Z., M. Van Horssen, S. Powell, and J. P. Garrahan, 2018, *Phys. Rev. Lett.* **121**, 040603.
- Landauer, R., 1961, *IBM J. Res. Dev.* **5**, 183.
- Landi, G. T., 2021, *Entropy* **23**, 1627.
- Landi, G. T., and M. Paternostro, 2021, *Rev. Mod. Phys.* **93**, 035008.
- Le, T. P., J. Levinsen, K. Modi, M. M. Parish, and F. A. Pollock, 2018, *Phys. Rev. A* **97**, 022106.
- Lenard, A., 1978, *J. Stat. Phys.* **19**, 575.
- Levitin, L. B., and T. Toffoli, 2009, *Phys. Rev. Lett.* **103**, 160502.
- Levy, A., L. Diósi, and R. Kosloff, 2016, *Phys. Rev. A* **93**, 052119.
- Lidar, D. A., and K. Birgitta Whaley, 2003, in *Irreversible Quantum Dynamics*, edited by F. Benatti and R. Floreanini, Lecture Notes in Physics Vol. 622 (Springer, Berlin), pp. 83–120.
- Lidar, D. A., I. L. Chuang, and K. B. Whaley, 1998, *Phys. Rev. Lett.* **81**, 2594.
- Liu, C., X. Chen, and L. Balents, 2018, *Phys. Rev. B* **97**, 245126.
- Liu, J., and G. Hanna, 2018, *J. Phys. Chem. Lett.* **9**, 3928.
- Liu, J., and D. Segal, 2021, *arXiv:2104.06522*.
- Liu, J., D. Segal, and G. Hanna, 2019, *J. Phys. Chem. C* **123**, 18303.
- Liu, J., D. Segal, and G. Hanna, 2021, *J. Phys. Chem. C* **125**, 7521.
- Liu, J. X., H. L. Shi, Y. H. Shi, X. H. Wang, and W. L. Yang, 2021, *Phys. Rev. B* **104**, 245418.
- Lu, W., J. Chen, L. M. Kuang, and X. Wang, 2021, *Phys. Rev. A* **104**, 043706.
- Lu, Z., and O. Raz, 2017, *Proc. Natl. Acad. Sci. U.S.A.* **114**, 5083.
- Macieszczak, K., M. Guta, I. Lesanovsky, and J. P. Garrahan, 2016, *Phys. Rev. Lett.* **116**, 240404.
- Macieszczak, K., D. C. Rose, I. Lesanovsky, and J. P. Garrahan, 2021, *Phys. Rev. Res.* **3**, 033047.
- Maffei, M., P. A. Camati, and A. Auffèves, 2021, *Phys. Rev. Res.* **3**, L032073.
- Maldacena, J., and D. Stanford, 2016, *Phys. Rev. D* **94**, 106002.
- Mandelstam, L., and I. Tamm, 1945, *J. Phys. (Moscow)* **9**, 249.
- Margolus, N., and L. B. Levitin, 1998, *Physica (Amsterdam)* **120D**, 188.
- Mattioni, A., F. Caycedo-Soler, S. F. Huelga, and M. B. Plenio, 2021, *Phys. Rev. X* **11**, 041003.
- Mazzoncini, F., V. Cavina, G. M. Andolina, P. A. Erdman, and V. Giovannetti, 2023, *Phys. Rev. A* **107**, 032218.
- Metzler, F., J. Sandoval, and N. Galvanetto, 2023, *arXiv:2303.01632*.
- Mikhnenko, O. V., P. W. Blom, and T. Q. Nguyen, 2015, *Energy Environ. Sci.* **8**, 1867.
- Mintert, F., A. Carvalho, M. Kus, and A. Buchleitner, 2005, *Phys. Rep.* **415**, 207.
- Mitchison, M., 2019, *Contemp. Phys.* **60**, 164.
- Mitchison, M. T., J. Goold, and J. Prior, 2021, *Quantum* **5**, 500.
- Modi, K., H. Cable, M. Williamson, and V. Vedral, 2011, *Phys. Rev. X* **1**, 021022.
- Mohan, B., and A. K. Pati, 2021, *Phys. Rev. A* **104**, 042209.
- Mondal, S., and S. Bhattacharjee, 2022, *Phys. Rev. E* **105**, 044125.
- Monsel, J., M. Fellous-Asiani, B. Huard, and A. Auffèves, 2020, *Phys. Rev. Lett.* **124**, 130601.
- Moraes, L. F., A. Saguia, A. C. Santos, and M. S. Sarandy, 2021, *Europhys. Lett.* **136**, 23001.
- Morrone, D., M. A. C. Rossi, and M. G. Genoni, 2023, *Phys. Rev. Appl.* **20**, 044073.
- Morrone, D., M. A. C. Rossi, A. Smirne, and M. G. Genoni, 2023, *Quantum Sci. Technol.* **8**, 035007.
- Müller, M. M., S. Gherardini, A. Smerzi, and F. Caruso, 2016, *Phys. Rev. A* **94**, 042322.
- Naidon, P., and S. Endo, 2017, *Rep. Prog. Phys.* **80**, 056001.
- Nandkishore, R., and D. A. Huse, 2015, *Annu. Rev. Condens. Matter Phys.* **6**, 15.
- Niedenzu, W., M. Huber, and E. Boukobza, 2019, *Quantum* **3**, 195.
- Ono, K., S. N. Shevchenko, T. Mori, S. Moriyama, and F. Nori, 2020, *Phys. Rev. Lett.* **125**, 166802.

- Oppenheim, J., M. Horodecki, P. Horodecki, and R. Horodecki, 2002, *Phys. Rev. Lett.* **89**, 180402.
- Ostroverkhova, O., 2016, *Chem. Rev.* **116**, 13279.
- Patel, A. A., and S. Sachdev, 2019, *Phys. Rev. Lett.* **123**, 066601.
- Peng, L., W. B. He, S. Chesi, H. Q. Lin, and X. W. Guan, 2021, *Phys. Rev. A* **103**, 052220.
- Pirmoradian, F., and K. Mølmer, 2019, *Phys. Rev. A* **100**, 043833.
- Place, A. P., *et al.*, 2021, *Nat. Commun.* **12**, 1779.
- Polini, M., *et al.*, 2022, [arXiv:2201.09260](https://arxiv.org/abs/2201.09260).
- Portmann, C., and R. Renner, 2022, *Rev. Mod. Phys.* **94**, 025008.
- Preskill, J., 2018, *Quantum* **2**, 79.
- Proesmans, K., J. Ehrich, and J. Bechhoefer, 2020, *Phys. Rev. Lett.* **125**, 100602.
- Pusz, W., and S. L. Woronowicz, 1978, *Commun. Math. Phys.* **58**, 273.
- Qi, S. F., and J. Jing, 2021, *Phys. Rev. A* **104**, 032606.
- Quach, J. Q., K. E. McGhee, L. Ganzer, D. M. Rouse, B. W. Lovett, E. M. Gauger, J. Keeling, G. Cerullo, D. G. Lidzey, and T. Virgili, 2022, *Sci. Adv.* **8**, 3160.
- Quach, J. Q., and W. J. Munro, 2020, *Phys. Rev. Appl.* **14**, 024092.
- Rodríguez, J. P. J., S. A. Chilingaryan, and B. M. Rodríguez-Lara, 2018, *Phys. Rev. A* **98**, 043805.
- Rodríguez, R. R., B. Ahmadi, P. Mazurek, S. Barzanjeh, R. Alicki, and P. Horodecki, 2023, *Phys. Rev. A* **107**, 042419.
- Rodríguez, R. R., B. Ahmadi, G. Suarez, P. Mazurek, S. Barzanjeh, and P. Horodecki, 2024, *New J. Phys.* **26**, 043004.
- Rosa, D., D. Rossini, G. M. Andolina, M. Polini, and M. Carrega, 2020, *J. High Energy Phys.* **11**, 067.
- Rossini, D., G. M. Andolina, and M. Polini, 2019, *Phys. Rev. B* **100**, 115142.
- Rossini, D., G. M. Andolina, D. Rosa, M. Carrega, and M. Polini, 2020, *Phys. Rev. Lett.* **125**, 236402.
- Roy, S., M. Landini, A. Trenkwalder, G. Semeghini, G. Spagnolli, A. Simoni, M. Fattori, M. Inguscio, and G. Modugno, 2013, *Phys. Rev. Lett.* **111**, 053202.
- Russo, M., K. E. McGhee, T. Virgili, D. G. Lidzey, G. Cerullo, and M. Maiuri, 2022, *Molecules* **27**, 7095.
- Sachdev, S., and J. Ye, 1993, *Phys. Rev. Lett.* **70**, 3339.
- Salvia, R., and V. Giovannetti, 2020, *Quantum* **4**, 274.
- Salvia, R., and V. Giovannetti, 2021, *Quantum* **5**, 514.
- Salvia, R., M. Perarnau-Llobet, G. Haack, N. Brunner, and S. Nimmrichter, 2023, *Phys. Rev. Res.* **5**, 013155.
- Santos, A. C., B. Çakmak, S. Campbell, and N. T. Zinner, 2019, *Phys. Rev. E* **100**, 032107.
- Santos, A. C., A. Saguia, and M. S. Sarandy, 2020, *Phys. Rev. E* **101**, 062114.
- Santos, A. C., and M. S. Sarandy, 2015, *Sci. Rep.* **5**, 15775.
- Schirhagl, R., K. Chang, M. Loretz, and C. L. Degen, 2014, *Annu. Rev. Phys. Chem.* **65**, 83.
- Scully, M. O., 2010, *Phys. Rev. Lett.* **104**, 207701.
- Seah, S., M. Perarnau-Llobet, G. Haack, N. Brunner, and S. Nimmrichter, 2021, *Phys. Rev. Lett.* **127**, 100601.
- Shaghghi, V., V. Singh, G. Benenti, and D. Rosa, 2022, *Quantum Sci. Technol.* **7**, 04LT01.
- Shaghghi, V., V. Singh, M. Carrega, D. Rosa, and G. Benenti, 2023, *Entropy* **25**, 430.
- Shi, H.-l., S. Ding, Q.-k. Wan, X.-h. Wang, and W.-l. Yang, 2022, *Phys. Rev. Lett.* **129**, 130602.
- Smerzi, A., 2012, *Phys. Rev. Lett.* **109**, 150410.
- Smyser, K. E., and J. D. Eaves, 2020, *Sci. Rep.* **10**, 18480.
- Son, J., P. Talkner, and J. Thingna, 2022, *Phys. Rev. A* **106**, 052202.
- Sone, A., and S. Deffner, 2021, *Entropy* **23**, 1107.
- Song, M. L., L. J. Li, X. K. Song, L. Ye, and D. Wang, 2022, *Phys. Rev. E* **106**, 054107.
- Tabesh, F. T., F. H. Kamin, and S. Salimi, 2020, *Phys. Rev. A* **102**, 052223.
- Taylor, N. B., and I. Kassal, 2018, *Chem. Sci.* **9**, 2942.
- Tejero, Á., J. Thingna, and D. Manzano, 2021, *J. Phys. Chem. C* **125**, 7518.
- Thingna, J., D. Manzano, and J. Cao, 2016, *Sci. Rep.* **6**, 28027.
- Tirone, S., R. Salvia, and V. Giovannetti, 2021, *Phys. Rev. Lett.* **127**, 210601.
- Touil, A., B. Çakmak, and S. Deffner, 2022, *J. Phys. A* **55**, 025301.
- Trudeau, R. J., 1994, *Introduction to Graph Theory* (Dover, New York).
- Uzdin, R., U. Günther, S. Rahav, and N. Moiseyev, 2012, *J. Phys. A* **45**, 415304.
- Uzdin, R., A. Levy, and R. Kosloff, 2016, *Entropy* **18**, 124.
- Vahala, K. J., 2003, *Nature (London)* **424**, 839.
- Vinjanampathy, S., and J. Anders, 2016, *Contemp. Phys.* **57**, 545.
- Vitanov, N. V., A. A. Rangelov, B. W. Shore, and K. Bergmann, 2017, *Rev. Mod. Phys.* **89**, 015006.
- von Lindenfels, D., O. Gräß, C. T. Schmiegelow, V. Kaushal, J. Schulz, M. T. Mitchison, J. Goold, F. Schmidt-Kaler, and U. G. Poschinger, 2019, *Phys. Rev. Lett.* **123**, 080602.
- Walton, Z. D., A. F. Abouraddy, A. V. Sergienko, B. E. A. Saleh, and M. C. Teich, 2003, *Phys. Rev. Lett.* **91**, 087901.
- Wang, B.-X., M.-J. Tao, Q. Ai, T. Xin, N. Lambert, D. Ruan, Y.-C. Cheng, F. Nori, F.-G. Deng, and G.-L. Long, 2018, *npj Quantum Inf.* **4**, 52.
- Wang, Y. K., and F. T. Hioe, 1973, *Phys. Rev. A* **7**, 831.
- Wells, N. P., and D. A. Blank, 2008, *Phys. Rev. Lett.* **100**, 086403.
- Wenniger, I. M. d. B., *et al.*, 2022, [arXiv:2202.01109](https://arxiv.org/abs/2202.01109).
- Wildeboer, J., T. Iadecola, and D. J. Williamson, 2022, *PRX Quantum* **3**, 020330.
- Wiseman, H. M., 1994, *Phys. Rev. A* **49**, 2133.
- Wiseman, H. M., and G. J. Milburn, 1993, *Phys. Rev. Lett.* **70**, 548.
- Wootters, W. K., 1981, *Phys. Rev. D* **23**, 357.
- Xu, K., H.-G. Li, Z.-G. Li, H.-J. Zhu, G.-F. Zhang, and W.-M. Liu, 2022, *Phys. Rev. A* **106**, 012425.
- Xu, K., H. J. Zhu, G. F. Zhang, and W. M. Liu, 2021, *Phys. Rev. E* **104**, 064143.
- Xu, K., H.-J. Zhu, H. Zhu, G.-F. Zhang, and W.-M. Liu, 2023, *Front. Phys.* **18**, 31301.
- Yan, J.-s., and J. Jing, 2023, *Phys. Rev. Appl.* **19**, 064069.
- Yang, D., S.-h. Oh, J. Han, G. Son, J. Kim, J. Kim, M. Lee, and K. An, 2021, *Nat. Photonics* **15**, 272.
- Yang, D.-L., F.-M. Yang, and F.-Q. Dou, 2023, [arXiv:2308.01188](https://arxiv.org/abs/2308.01188).
- Yang, H.-Y., H.-L. Shi, Q.-K. Wan, K. Zhang, X.-H. Wang, and W.-L. Yang, 2024, *Phys. Rev. A* **109**, 012204.
- Yang, T.-R., Y.-Y. Zhang, H. Dong, L. Fu, and X. Wang, 2020, [arXiv:2010.09970](https://arxiv.org/abs/2010.09970).
- Yang, X., Y.-H. Yang, M. Alimuddin, R. Salvia, S.-M. Fei, L.-M. Zhao, S. Nimmrichter, and M.-X. Luo, 2023, *Phys. Rev. Lett.* **131**, 030402.
- Yao, Y., and X. Q. Shao, 2021, *Phys. Rev. E* **104**, 044116.
- Yao, Y., and X. Q. Shao, 2022, *Phys. Rev. E* **106**, 014138.
- Zakavati, S., F. T. Tabesh, and S. Salimi, 2021, *Phys. Rev. E* **104**, 054117.
- Zanardi, P., and M. Rasetti, 1997, *Phys. Rev. Lett.* **79**, 3306.
- Zhang, X., and M. Blaubaer, 2023, *Front. Phys.* **10**.

- Zhang, Y. Y., T. R. Yang, L. Fu, and X. Wang, 2019, *Phys. Rev. E* **99**, 052106.
- Zhao, F., F. Q. Dou, and Q. Zhao, 2021, *Phys. Rev. A* **103**, 033715.
- Zhao, F., F. Q. Dou, and Q. Zhao, 2022, *Phys. Rev. Res.* **4**, 013172.
- Zhen, Y.-Z., D. Egloff, K. Modi, and O. Dahlsten, 2021, *Phys. Rev. Lett.* **127**, 190602.
- Zhong, X., T. Chervy, S. Wang, J. George, A. Thomas, J. A. Hutchison, E. Devaux, C. Genet, and T. W. Ebbesen, 2016, *Angew. Chem., Int. Ed.* **55**, 6202.
- Zueco, D., F. Galve, S. Kohler, and P. Hänggi, 2009, *Phys. Rev. A* **80**, 042303.
- Zutshi, A., and D. Goswami, 2021, *Int. J. Inf. Manage. Data Insights* **1**, 100042.